

UNCLASSIFIED

AD NUMBER

ADB014768

LIMITATION CHANGES

TO:

Approved for public release; distribution is unlimited.

FROM:

Distribution authorized to U.S. Gov't. agencies only; Administrative/Operational Use; FEB 1976. Other requests shall be referred to Naval Air Systems Command, Arlington, VA.

AUTHORITY

NAVAIR ltr 4 Nov 1977

THIS PAGE IS UNCLASSIFIED

THIS REPORT HAS BEEN DELIMITED
AND CLEARED FOR PUBLIC RELEASE
UNDER DOD DIRECTIVE 5200.20 AND
NO RESTRICTIONS ARE IMPOSED UPON
ITS USE AND DISCLOSURE.

DISTRIBUTION STATEMENT A

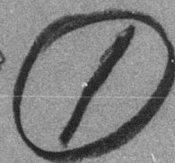
APPROVED FOR PUBLIC RELEASE;
DISTRIBUTION UNLIMITED.

ADB014768

UNCLASSIFIED

R76-912024-8

A METHOD FOR COMPUTING THREE-DIMENSIONAL VISCOUS FLOWS OVER AN OGIVAL BODY AT ANGLE OF ATTACK (U)



Final Report

(19 Sept 74 to 18 Oct 75)

By

P.R. Eiseman

and

R. Levy

DISTRIBUTION LIMITED TO U.S.
GOVERNMENT AGENCIES ONLY:

☐ FOREIGN INFORMATION

☐ PRELIMINARY INFORMATION

☒ TEST AND EVALUATION

☒ CONTRACTION PERFORMANCE EVALUATION

DATE: 11/9/76

OTHER REQUESTS FOR THIS DOCUMENT

MUST BE REFERRED TO COMMANDER,

NAVAL AIR SYSTEMS COMMAND, AIR-554

Prepared Under Contract N00019-75-C-0097

for

Naval Air Systems Command
Department of the Navy

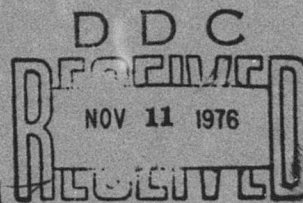
by

**UNITED TECHNOLOGIES
RESEARCH CENTER**



UNITED
TECHNOLOGIES

EAST HARTFORD, CONNECTICUT 06108



B

UNCLASSIFIED

R76-912024-8

A Method for Computing Three-Dimensional Viscous Flows
Over an Ogival Body at Angle of Attack

TABLE OF CONTENTS

	<u>Page</u>
ABSTRACT	1
INTRODUCTION	2
THE METRIC TENSOR AND ITS RELATIONSHIP TO SYSTEMS OF COORDINATES	7
THE GENERAL FORMATION OF AN INITIAL VALUE PROBLEM FOR STRONGLY CONVECTIVE FLOWS	11
THE NUMERICAL METHOD	17
Overview	17
The System of Equations	18
The Numerical Scheme	21
THE COORDINATE SYSTEM	29
The Construction of Tube-Like Coordinates	29
The Length Factor	32
The Construction of Bounding Tubes	34
Distribution Functions.	35
Metric Data for Tube-Like Coordinates	36
TREATMENT OF THE BOW SHOCK	47
REFERENCES	48

(See 1473)

ADDITIONAL	
RTM	White Section <input type="checkbox"/>
CS	Buff Section <input checked="" type="checkbox"/>
UNANNOUNCED	<input type="checkbox"/>
JUSTIFICATION	
BY	
DISTRIBUTION/AVAILABILITY CODES	
Doc.	AVAIL. and/or SPECIAL
B	

ABSTRACT

A method for computing three-dimensional flow over an ogival body at angle of attack is described. An approximate set of governing equations is derived for viscous flows which have a primary flow direction. The derivation is done in a coordinate independent manner, and the resulting equations are expressed in terms of tensors. In keeping with the inherent generality of the tensor formulation, a two-level second-order accurate marching procedure is derived for general tensor-like equations. With this procedure, a three-dimensional turbulent flow can be solved in any coordinate system by marching along the assumed primary flow direction. General tube-like coordinates are developed for a class of geometries applicable to flows between tubular surfaces. The coordinates are then particularized to the flow field bounded between an ogival body at angle of attack and its bow shock. Unlike the ogival body surface, the bow shock surface is not known in advance of the solution but instead must be computed as the solution develops. One marching step of the solution process is broken down into several steps. First, the bow shock surface is discretely extended by an iteration of explicit local solutions. The bow shock surface is then smoothly extended to provide a best fit to the discrete shock data. Tube-like coordinates are generated and finally the second order numerical scheme is applied to advance the fully viscous solution to the next station.

A Method for Computing Three-Dimensional Viscous Flows
Over an Ogival Body at Angle of Attack

INTRODUCTION

An important consideration in the design of supersonic missiles is the accurate prediction of both the pressure distribution and heat transfer loads about the body. Although the combination of inviscid flow theory and three-dimensional boundary layer theory may be adequate to predict the flows about ogival bodies at small angles of attack, these analyses used separately are inadequate at larger angles of attack. At larger angles of attack, a strong viscous-inviscid interaction occurs on the lee side of the body leading to the formation of a pair of vortices symmetric about the lee body generator and an accurate flow field prediction under these conditions requires a solution which considers the mutual interaction between the viscous layer and the nominally inviscid flow. Since increases in the body lift to drag ratio and in local heat transfer rate on the lee side of the body are associated with the formation of the vortices, an accurate method of predicting the lee side interacting flow field is necessary to insure both the effective operation and structural integrity of supersonic vehicles.

Successful predictions of the flow about ogival bodies at angle of attack require an accurate flow model in which the strong viscous-inviscid coupling on the lee side of the vehicle at large angle of attack is modeled correctly. Boundary layer theory is not adequate to describe the development of viscous flow phenomena as complex as vortex rollup since the basic assumption that the boundary layer is thin compared to a typical body scale is invalid. Thus, a three-dimensional interacting boundary layer theory would be inadequate for description of the problem. Although a numerical solution to the full Navier-Stokes equations would provide a theory with the necessary generality to successfully predict such complex flows, the required computer time and storage indicate that three-dimensional Navier-Stokes solutions should be used only if no suitable alternative exists. An optimum analysis would possess the general three-dimensional nature of the Navier-Stokes equations but would not be limited by the large running time and storage requirements associated with three-dimensional Navier-Stokes solutions.

The problem of predicting the flow field about sharp nosed ogival bodies at incidence has been under investigation for the designer in his consideration of aerodynamic forces and heating loads. At supersonic speeds the flow over ogival bodies at incidence may be thought of as having a component aligned with the free-stream flow direction, which is little affected by viscous forces, and cross flow components flowing around the body, which can, at large angles of attack, become

viscous dominated. This picture of ogival flow fields is borne out by various experimental investigations (see Refs. 1, 2, 3, and 4). These investigations have found that at zero angle of attack a symmetric flow field develops about the body, in which no cross flows exist. As the angle of attack is increased from zero, a cross flow pattern begins to develop proceeding from the windward symmetry plane toward the leeward symmetry plane. When the angle of attack becomes large enough, the cross flow adverse pressure gradient existing near the lee symmetry plane becomes sufficiently strong and the cross flow separates, leading to the development of a pair of vortices symmetric about the lee symmetry plane as depicted in Fig. 1. These vortices may or may not have imbedded shocks associated with them. The flow as depicted in Fig. 1 has been verified for both laminar and turbulent flows for speeds in the supersonic and hypersonic regimes. The available experimental data indicates that flow separation (reversal) in the axial direction usually is not associated with the vortex development.

The majority of previous attempts to predict flows of this type may be categorized as either solutions of the inviscid flow equations or solutions to the three-dimensional boundary layer equations. Even with the simplifying assumptions of these two approaches the equations must still be solved numerically. Furthermore, most previous investigations have been limited to the problem of flow over conical bodies in which axial invariance is assumed in order to eliminate derivatives in the direction of the cone axis. Such analyses cannot be used to analyze general body shapes or to accurately predict the development of the lee side vortices.

The most common inviscid procedure currently in use involves numerical solution of the time-dependent inviscid flow equations. The steady inviscid flow solution is approached asymptotically for large values of time. The solutions of Moretti (Refs. 5 and 6) are examples of this type of approach. Other available inviscid techniques include the inverse method (Ref. 7) and the method of integral relations (Ref. 8). MacCormack and Warming (Ref. 9) have recently surveyed the available inviscid computational procedures. An obvious disadvantage of a purely inviscid solution to this problem is the failure to account for viscous effects. Viscous forces may be accounted for, however, by making use of the inviscid pressure distribution to solve the three-dimensional boundary layer equations (see Ref. 10). This procedure can give accurate predictions of ogival flow fields provided the angle of attack is small enough to prevent cross flow separation and hence does not permit lee side vortices. However, the small angle of attack constraint places a severe restriction on the boundary layer type procedures.

Because of their complexity, and particularly the interaction which occurs between primary and secondary flows and viscous and inviscid regions, three-dimensional flows over ogival bodies at nontrivial angles of attack have been extremely difficult to analyze. There are considerable difficulties associated with the synthesis of inviscid flow analysis and boundary layer theory into a cohesive method of analysis. Among these difficulties are the lack of applicability of

three-dimensional boundary layer theory, a means for patching or interfacing boundary layer and rotational inviscid flow regions, and the treatment of interaction between viscous and inviscid flow regions.

In efforts to develop methods for dealing with problems of this type, Patankar & Spalding (Ref. 11), Caretto, Curr, & Spalding (Ref. 12), and Briley (Ref. 13) devised numerical methods for solving approximate governing equations which are a more or less natural generalization of three-dimensional boundary layer theory. In these studies, solutions were computed for laminar incompressible flow in straight ducts with rectangular cross sections. The governing equations were solved by integrating in a primary flow coordinate direction while retaining viscous stresses in both transverse coordinate directions as opposed to only one direction for three-dimensional boundary layer theory. In addition, certain assumptions were made about the behavior of pressure gradient terms for incompressible flow to permit solution by forward marching integration. Subsequently, this general approach has been used to compute laminar incompressible flow in helical tubes by Patankar, Pratap, & Spalding (Ref. 14). A predictor/corrector solution procedure has been developed by Lin and Rubin (Refs. 15 and 16) to solve the parabolized three dimensional compressible Navier Stokes equations. The numerical technique is implicit in one transverse direction and iterative in the other. Helliwell and Lubard (Ref. 17), Rakich and Lubard (Ref. 18), and Lin and Rubin (Ref. 16) have applied this method to the problem of flow over both sharp and spherically blunted cones at angle of attack.

Recently in companion studies, Briley & McDonald (Ref. 19) and McDonald & Briley (Ref. 20) have developed stable and efficient noniterative implicit numerical techniques for application to systems of coupled nonlinear multidimensional nonelliptic equations. These general techniques were applied by McDonald & Briley (Ref. 20) to the computation by forward marching integration of laminar supersonic flow in rectangular jets. Subsequently, the laminar incompressible straight-duct analysis of Briley (Ref. 13) and the improved numerical techniques of McDonald & Briley (Ref. 20) for compressible flows were extended and synthesized by Briley & McDonald (Ref. 21) and Eiseman, McDonald, and Briley (Ref. 22) into a method for computing subsonic turbulent flow in curved ducts. The present study represents a further generalization of the latter method, to encompass general coordinates and highly complex geometries.

In the ogival body problem the basic geometry is determined by both the ogival body itself and by the bow shock propagated from the tip of the body. Unlike the body shape, the bow shock is not known in advance, but must be determined as part of the solution. Since the region nearest the shock is dominated by convective forces, and the shock is treated as a discontinuity, it is quite sufficient to perform a local inviscid analysis in that region; and, thereby, to determine the shock location one step in advance of the fully viscous solution which is being marched along the axis of the ogival body. The shock location is calculated numerically in terms of local extensions of the existing coordinate system. In this way

each new point of shock location can be explicitly computed independent of neighboring transverse points; and, hence, remove any need to construct a potentially costly global coordinate extension which would ultimately be discarded. Specifically, for each new shock point we have a distinctly tailored coordinate system which is an extension of the previous coordinate system that encompasses only the explicit difference molecule for the point in question. A distinct advantage here is that the metric data necessary to write the appropriate equations must only be determined at the shock point in question since the metric data at the explicit level is already in storage from the previous step. After the shock data has been determined one is left with a loop of points one station ahead of a smooth shock surface. The problem now is to extend the shock surface in a sufficiently smooth and uniform manner so that suitable coordinates can be generated for the advancement of the fully viscous solution to the same axial location of the just completed shock calculation. The loop of shock points may lack a certain amount of uniformity by having oscillations in curvature if a strict interpolation were to be performed. The lack of uniformity can easily arise from the numerical nature of the calculation. Thus a least-squares spline procedure is employed to remove the noisy oscillations of the data and to produce a loop which is smooth enough to possess continuous third derivatives (needed for a viscous calculation) and uniform enough to have curvature which reflects the global structure of the shock surface. At this point one has a well-defined loop in front of a well-defined surface. The surface is now easily extended in a patchwise fashion by smoothly joining polynomial surface elements. From here the coordinates are generated by a linear deformation of the ogival body surface into the bow shock surface. The rate of deformation is controlled by a choice of the linear deforming parameter. This parameter is constrained to monotonically and smoothly vary from zero to unity. As this variation occurs, a family of coordinate surfaces is generated from the ogival body to the bow shock. When the parameter is chosen to be a function of only the deforming direction, the deformation is uniform over the body surface. This is ideal for global resolutions over or within an object. If, in addition, the deformation parameter should also depend upon surface location, then local resolutions would be possible. In the ogival body problem, however, the global resolutions are sufficient to adequately resolve the large velocity gradients associated with the attached boundary layer.

Throughout the discussion to follow the material will be ordered from the more general to the more specific. In so doing one has more flexibility and generality at hand to apply to the ogival body problem. Thus it is best to start off with a discussion on the rationale behind the use of curvilinear coordinate systems for fluid dynamic problems. While the application of various coordinate systems is not a new idea, the coordinate independent concept associated with analyses based upon the metric tensor is of greater utility. The metric tensor, as developed in the initial discussion, is used to compare coordinate systems of varying degrees of generality. In the next section use is made of the metric tensor to obtain a tensor (coordinate independent) form of the Navier-Stokes Equations which are then approximated to produce an initial value problem. The approximation is obtained from a

neglect of viscous stresses, and hence diffusion, in an assumed primary flow direction. The approximation can be viewed as a generalization of boundary layer theory. The primary flow direction is assumed to be given by some smooth vector field. Since the specification of any vector field is independent of coordinates, the approximation of the tensor form of the Navier-Stokes equations is also independent of coordinates. As a matter of convenience, however, the primary vector field is often chosen to be the vector field associated with a given coordinate direction of a given system of coordinates. For the ogival body problem this is done. To maintain the generality of the discussion one next considers the general numerical method rather than the details of coordinate generation. This is consistent with this general methodology since the computer code is constructed in a modular fashion in terms of the metric data. After this discussion one considers the construction of coordinates that are suitable for the ogival body problems; however, some generality is still maintained by considering coordinate systems that are generated from any two concentric tubes. The metric data is then obtained so that the arbitrary two tube problem is fully specified once the tubes are specified. In the present study the inner tube is taken to be the ogival body and the outer tube is taken to be the bow shock. One finally considers the numerical generation of bow shock data, and the use of that data to suitably extend the bow shock surface so that a well-defined outer tube is specified.

THE METRIC TENSOR AND ITS RELATIONSHIP TO SYSTEMS OF COORDINATES

The governing equations for a viscous fluid will be expressed and approximated in generalized coordinates. Like any physical process, the dynamics of a fluid is independent of coordinates; and is, therefore, describable in terms of arbitrary coordinates. The practical implication of this coordinate independence is that the analyst has the freedom to select coordinate systems which are easy to construct and which simplify the solution process.

In the numerical solution of fluid dynamic problems there are many advantages to be gained by judicious choice of coordinates. The most obvious advantage is that the physical boundaries of a flow region can be represented by coordinate surfaces. This removes the need for fractional cells and hence removes the complications and loss of accuracy associated with an interpolation algorithms for the boundaries. Another advantage in the use of generalized coordinates is that a uniform numerical method can be used. The solution can then be performed with a fixed number of cells in any given direction and with a uniform mesh spacing. The result is a simplification of the computer logic; and hence, a savings in time for both the computer and the programmer. For the ADI method of solution that we use, the one-dimensional rows and columns each have fixed lengths; and hence, we are not faced with the combinatorial problem of monitoring the lengths of rows and columns which would otherwise be caused by geometric changes in the boundaries. In addition to the above there is the advantage of an implicit mesh distribution. The uniform mesh of computational space is simply mapped into an appropriately distributed mesh in physical space. Thus, the coordinate transformation can be chosen to contain the distributional information as well as the boundary specifications. The resolution of a rapidly changing solution is the major objective in selection of a coordinate mesh distribution. A classical example is the resolution of attached boundary layers where the solution is known to have large velocity gradients. Another more subtle example is the resolution of large gradients in computational coordinates due to regions of high curvature on the bounding surfaces. When the transformation contains the distributional information there is no need to construct the apparatus for the discrete approximation of derivatives on a nonuniform mesh. This is a savings in both computer logic and storage. With a different motivation, however, it may be desired to automate the difference molecule so that the numerical technique can be changed with a few parameters. Changes, in practice, usually amount to a selection between forward, backward or central differences. For any given direction we need three parameters for first derivatives and three parameters for second derivatives. Thus, even with such an automation of the numerical method we save on computer logic and storage. Specifically, for an ADI direction of length N we need only 12 parameters as opposed to $6N$ parameters for nonuniform meshes. The extra 6 parameters are for the boundary molecules. A further advantage is that for a given problem we can select coordinates from a large class of coordinate systems. In the process of sorting through the various possible coordinate systems we are guided by two criteria. First, the new coordinates must lead to a real simplification; and secondly, the coordinates must be

easily generated. Since bounding surfaces usually become coordinate surfaces the first criterion is directly measured by consideration of the metric tensor (g_{ij}) which is obtained from the expression for the fundamental element of arc length

$$(ds)^2 = g_{ij} dy^i dy^j \quad (1)$$

Specifically, an increase in the number of nontrivial elements in the expression of the metric tensor is accompanied by a corresponding increase in the number of terms in the equations of motion. The result is an increase in the computational work that is needed after the coordinates have been generated along with the necessary metric data. The second criterion, unlike the first, is most often neglected. The unfortunate result is that there is often more work involved in making the coordinates than in solving the original problem with a less efficient satisfaction of the first criterion. In fact, both of the criteria above usually are at opposite polarities in complexity. The prudent selection of coordinates is then a balance between these criteria.

Our criteria for selecting a suitable system of coordinates can be used to compare the various classes of coordinate systems and to evaluate the relative utility of each. We will start with conformal transformations and continually enlarge the class until we obtain general nonorthogonal coordinates.

For conformal transformations the metric tensor is simply given by a scalar multiple of the identity. That is, $g_{ij} = h(\vec{y}) \delta_{ij}$ where the kronecker symbol δ_{ij} vanishes unless $i = j$ in which case it is unity. From this expression it is easy to show that $h = (J^2)^{1/n}$ where J is the Jacobian of the n -dimensional conformal transformation. The simplicity of the metric leads to very simple equations of motion at the expense of greatly restricting the class of easily obtained transformations. These transformations are generally obtained by the solution of partial differential equations which may in itself be costly. In addition, the control over the mesh distributions is indirect at best. In two dimensions, however, conformal transformations have been successfully used on many occasions. Here the metric is given by $g_{ij} = |J| \delta_{ij}$, and the theory of functions of one complex variable is a powerful tool that is at our disposal. When the boundaries of the flow region can be matched with well-known conformal transformations there is nothing that can effectively compete with this way of generating coordinates. We have simply optimized on the generation of the equations of motion and on their solution process for any given method of solution. In a number of cases boundaries can be matched through a sequence of well-known transformations. However, in most cases of practical importance the boundaries are too complicated; and consequently, cannot be simply defined as desired.

When conformal mappings become overly difficult to construct, it is best to consider the slightly larger class of orthogonal transformations. For orthogonal transformations the metric tensor is given by the diagonal form $g_{ij} = [h_i(y)]^2 \delta_{ij}$.

Note that, unlike the conformal transformations, the diagonal entries of the metric can be different. The deviation from conformality can now easily be measured by an examination of the ratios of the functions h_i . To see why this is so we need an explicit geometric interpretation of the metric. For a position vector field \vec{x} , the vector field $\vec{e}_i = \partial \vec{x} / \partial y^i$ is the natural tangent vector field along coordinate curves generated by holding the remaining coordinates $y^1, \dots, y^{i-1}, y^{i+1}, \dots, y^n$ constant. It is often common practice to use the operator notation where the position vector field is omitted. By an application of the chain rule, the fundamental element of arc length can be expanded as

$$(ds)^2 = d\vec{x} \cdot d\vec{x} = \left(\frac{\partial \vec{x}}{\partial y^i} dy^i \right) \cdot \left(\frac{\partial \vec{x}}{\partial y^j} dy^j \right) = \frac{\partial \vec{x}}{\partial y^i} \cdot \frac{\partial \vec{x}}{\partial y^j} dy^i dy^j = (\vec{e}_i \cdot \vec{e}_j) dy^i dy^j \quad (2)$$

and hence, by linear independence $g_{ij} = \vec{e}_i \cdot \vec{e}_j$. Now note that we have an orthogonal metric if and only if the \vec{e}_i and \vec{e}_j are perpendicular when $i \neq j$. But perpendicularity of \vec{e}_i and \vec{e}_j at a point is equivalent to the perpendicular crossing of the associated coordinate curves at the point in question. Consequently our intuitive notion of orthogonality in terms of coordinate curves is equivalent to the metric expression above. In addition the functions h_i are easily seen to be equal to the lengths of the corresponding natural tangent vectors \vec{e}_i . In a small neighborhood of a point the functions h_i are nearly equal to their values at the point and thus, the measurement of distance along coordinate curves is very nearly given by distance measurements along the respective vectors \vec{e}_i in the tangent plane at the point in question. When the functions h_i are all equal, the distance measurement in the tangent plane is merely a uniform dilation or contraction of the original cartesian system. Thus, length ratios and, hence, angles are preserved between the cartesian system and the tangent plane. But the projection of tangent vectors onto the curvilinear system preserves angles. Hence, with equal diagonal entries the transformation preserves angles and is, therefore, called conformal. Consequently, as the ratios of the h_i deviate from unity, the transformation smoothly deviates from conformality. With fewer constraints on the metric the selection of coordinates from the class of orthogonal transformations is slightly less restrictive than a selection from the class of conformal transformations. The process of coordinate generation is usually accomplished by geometric methods which result in a system of differential equations. The solution of these equations is often too costly to reasonably perform just to obtain coordinates. In addition, it may be difficult or even impossible to properly distribute mesh points and still preserve orthogonality.

General nonorthogonal coordinates are often to be preferred since the mesh distributions can be controlled and since the coordinates are considerably easier to generate. The construction process is entirely geometric and generally does not rely on the solution of differential equations. Furthermore, points can be essentially distributed at will. Mesh distribution functions can often be directly inserted into the transformation in a manner which directly distributes the points. The considerable

improvement in flexibility associated with the class of general spacial coordinates does come with a small price. Specifically, the metric tensor has generally non-trivial off diagonal elements. As with the difference between orthogonal and conformal coordinates, the deviation of the general nonorthogonal coordinates from orthogonality can be measured directly from the metric. That is, the cosine of the angle between distinct coordinate curves is given by the dot product of the associated unit tangent vectors. The cosine of the angle between curves i and j can be written as:

$$\left(\frac{\vec{e}_i}{|\vec{e}_i|} \right) \cdot \left(\frac{\vec{e}_j}{|\vec{e}_j|} \right) = \frac{\vec{e}_i \cdot \vec{e}_j}{\sqrt{(\vec{e}_i \cdot \vec{e}_i)(\vec{e}_j \cdot \vec{e}_j)}} = \frac{g_{ij}}{\sqrt{g_{ii} g_{jj}}} \quad (3)$$

Thus when g_{ij} vanishes for distinct i and j we have orthogonality, and when g_{ij} increases from 0 the coordinates smoothly deviate from orthogonality with deviation given by the arc cosine of the above. This deviation can be used to advantage by creating almost orthogonal coordinates in certain regions of importance. For example, one may wish to treat boundary layers with nearly orthogonal coordinates and let regions of greater nonorthogonality fall into largely inviscid regions.

With all of the above considerations born in mind it is clear that the general nonorthogonal coordinates are the most suitable choice for the numerical calculation of the fully viscous flow field over an ogival body at angle of attack. In particular the tube-like coordinate systems to be discussed in a later section are general non-orthogonal coordinates which are ideally suited to the ogival body problem. Coordinate generation with tube-like coordinates is computationally efficient and at the same time is flexible enough to allow for a great degree of control over the mesh distribution. This control is needed for the resolution of boundary layers and other regions where large gradients occur. The basic choice of these nonorthogonal coordinates essentially places the emphasis on the fluid dynamic problem rather than on the generation of coordinate systems per se.

THE GENERAL FORMATION OF AN INITIAL VALUE PROBLEM FOR STRONGLY CONVECTIVE FLOWS

Central to the present analysis is the formulation of approximate governing equations which can be solved by forward marching integration in the direction of a "primary flow". The entire flow field can thereby be obtained by a sequence of essentially two-dimensional calculations. This feature of the method results in a substantial saving of computer time and storage compared to that which would be required for solution of the full Navier-Stokes equations. The equations are derived in a coordinate independent manner. A vector field that reasonably approximates the primary flow direction is chosen and then used as the basis for an approximation of the stress tensor. The time-averaged equations are written in general conservation law form, and then the approximate stress tensor is inserted to obtain the approximate equations. Note that this process depends only on the choice of a primary vector field, and not on the particular coordinate system used for the numerical solution. The primary vector field used here consists of the tangent vectors to a certain family of coordinate curves that are roughly aligned with the flow geometry.

The governing equations are derived from the Navier-Stokes equations for compressible flow of a viscous, perfect gas. In conservation law form (Ref. 23) and, in general curvilinear coordinates (y^1, y^2, y^3) , these equations are given by

$$\frac{\partial \rho}{\partial t} + \frac{\partial}{\partial y^i} (\rho v^i \sqrt{g}) = 0 \quad (4a)$$

for continuity and

$$\frac{\partial}{\partial t} \left[\rho v^i \frac{\partial x^s}{\partial y^i} \sqrt{g} \right] + \frac{\partial}{\partial y^j} \left[(\rho v^i v^j + \tau^{ij}) \frac{\partial x^s}{\partial y^i} \sqrt{g} \right] = 0 \quad (4b)$$

for momentum. Constant total temperature is assumed, and thus an energy equation is not required. We have used (x^1, x^2, x^3) for fixed cartesian coordinates, ρ , for density,

$\vec{v} = v^k \vec{e}_k$ for velocity, $g = \det(g_{ij}) = \left| \det \left(\frac{\partial x^i}{\partial y^j} \right) \right|^2$ for the metrical determinant, and τ^{ij} for the components of the stress tensor in the basis $\vec{e}_i \otimes \vec{e}_j$. In terms of the metric, the components of the stress tensor are given by

$$\tau^{ij} = g^{ij} p + \alpha_k^{ij} v^k + \beta_k^{ij} \frac{\partial v^k}{\partial y^l} \quad (5a)$$

where

$$\alpha_k^{ij} = \mu \left(\frac{2}{3} g^{ij} \Gamma_{kl}^l + \frac{\partial g^{ij}}{\partial y^k} \right) \quad (5b)$$

and

$$\beta_k^{ijl} = \mu \left(\frac{2}{3} g^{ij} \delta_k^l - g^{il} \delta_k^j - g^{jl} \delta_k^i \right) \quad (5c)$$

for viscosity μ , inverse metric g^{il} , Kronecker deltas $\delta_j^i = \delta^{ij} = \delta_{ij}$, and Christoffel symbols

$$\Gamma_{ij}^k = \frac{g^{km}}{2} \left\{ \frac{\partial g_{im}}{\partial y^j} + \frac{\partial g_{jm}}{\partial y^i} - \frac{\partial g_{ij}}{\partial y^m} \right\} \quad (5d)$$

From the ideal gas law and the constant total temperature assumption, the perfect gas relation has the form

$$p = A\rho + B\rho g_{ij} v^i v^j$$

where A and B are constants. In all of the above, the Einstein summation convention is assumed. That is, matching upper and lower indices are to be summed from 1 to 3 unless otherwise stated.

It is assumed that for high Reynolds number, viscous effects are negligible except in thin layers near the walls, and thus boundary layer concepts can be employed to examine the relative importance of viscous terms in the governing equations. Consequently, viscous terms which are considered important for boundary layer flow on walls are retained; other viscous terms are neglected. In this sense, the present approach can be regarded as a natural extension of three-dimensional boundary layer theory. Unlike conventional boundary layer theory, however, the approximate equations are to be applicable in the inviscid flow region as well as the viscous region and, thus, no approximations are made for inviscid terms other than those to be used for the pressure field in subsonic flow.

To account for turbulent transport processes, the governing equations are time-averaged in the usual manner for turbulent flows (e.g., Hinze, Ref. 24). This process of averaging produces turbulent correlations which are conventionally termed Reynolds stresses. Certain components of viscous stress are removed from the time-averaged equations. The process of viscous approximation is based upon the assumption that a primary flow direction exists. This direction is assumed to be given in the form of

a vector field $\vec{\xi}_3$ which identifies a direction at each spatial point. Then $\vec{\xi}_3$ can be extended to an orthogonal triple of vectors $\vec{\xi}_1, \vec{\xi}_2, \vec{\xi}_3$ at each spatial point. This extension must be accomplished in a smooth enough fashion over the whole flow field so that at least one derivative can be taken. The required differentiability occurs because of the requirement to differentiate the components of the stress tensor as they occur in the Navier-Stokes equations. From this construction one obtains a specification of a field of orthogonal frames where $\vec{\xi}_3$ is aligned with the assumed primary flow direction, and for each point $\vec{\xi}_1$ and $\vec{\xi}_2$ span an orthogonal transverse plane. Within such a frame, we form a differential viscous stress cube (Fig. 2). The resulting components of viscous stress on the cube surface are either aligned with or are orthogonal to the primary direction. In this way the force balances represented by the Navier-Stokes equations are effectively separated into three mutually exclusive directions so that approximations in any given direction do not directly affect other directions. That is, forces in any one of the directions do not have nontrivial projections on the other two remaining directions. If the equations of motion were written for the isolated cube, then the stress components would contribute to the force balance in their respective directions. However, in the primary direction $\vec{\xi}_3$, the viscous contribution $\vec{\sigma}^{33}$ is expected to add little to the strong convective forces and, hence, this contribution is ignored. In addition, the contribution of the viscous shearing stresses $\vec{\sigma}^{31}$ and $\vec{\sigma}^{32}$ to the force balance in the transverse equations for the $\vec{\xi}_1$ and $\vec{\xi}_2$ directions is also small relative to convective forces. These force balances are mutually exclusive due to the orthogonality of the frame. Effectively, we can generate longer and longer viscous stress cubes by joining existing cubes along transverse faces. The total assumption is that viscous forces on transverse faces are negligible. Eventually, we are considering forces on a fiber-like object aligned with the primary direction (Fig. 2). From this viewpoint, we are just neglecting internal viscous forces within the fiber. That is, the fiber has no stiffness and, therefore, the only balance against the convective forces is due to the shearing stress along its boundary. This is particularly appropriate when the fiber is in the boundary layer, where the no-slip condition causes the fluid to decelerate and come to rest at the walls.

For a viscous stress cube in the frame $\vec{\xi}_1, \vec{\xi}_2, \vec{\xi}_3$, the viscous stresses have the form

$$\vec{\sigma}^{ij} = \vec{\sigma}^{ij} \vec{\xi}_i \otimes \vec{\xi}_j \quad (6)$$

and it is postulated that the components $\vec{\sigma}^{3i}$ for $i = 1, 2, 3$ are negligible relative to convective forces. Thus we shall replace the tensor $\vec{\sigma}^{ij} \vec{\xi}_i \otimes \vec{\xi}_j$ with the tensor $\tilde{\sigma}^{ij} \vec{\xi}_i \otimes \vec{\xi}_j$ where $\tilde{\sigma}^{ij} = (1 - \delta_i^3) \sigma^{ij}$. Unlike the original tensor, this new tensor is not symmetric. When this is inserted into the time-averaged Navier-Stokes equations, we obtain an approximate set of governing equations which are not elliptic, and which can be solved by a forward marching procedure.

The approximate governing equations are obtained in terms of the metric data associated with a curvilinear coordinate system. In the ogival body problem, tube-like coordinates are used to match coordinate surfaces with the ogival body and the bow shock. The solution is obtained by a forward marching procedure down the axis of the ogival body. The development and analysis of tube-like coordinates is presented in a later section, together with the metric data. For the present, we will assume that we are given an arbitrary coordinate direction taken as a marching direction for the solution. This direction need not be aligned with the primary flow direction ξ_3 . The natural basis of vectors tangent to coordinate curves is given by $\vec{e}_i = \partial/\partial y^i$ for $i = 1, 2, 3$. But the basis $\vec{\xi}_1, \vec{\xi}_2, \vec{\xi}_3$, for our approximations is independent of this coordinate basis. Hence, our approximation scheme is executed by transformation of the viscous stress from the \vec{e}_i basis into $\vec{\xi}_i$, followed by the stress approximation as described above and, finally, a transformation from the $\vec{\xi}_i$ basis back into \vec{e}_i . This requires the transformation $\vec{\xi}_j = \xi_j^i \vec{e}_i$ and its inverse $\vec{e}_i = \eta_i^k \vec{\xi}_k$. In the Navier-Stokes equations, the components of stress are represented by a sum

$$\tau^{ij} = p g^{ij} + v^{ij} \quad (7)$$

where v^{ij} is the viscous part of the stress tensor. But the τ^{ij} are just the coefficients of the stress tensor $\tau^{ij} \vec{e}_i \otimes \vec{e}_j$ in the natural basis of tangents to coordinate curves. Thus we must express its viscous part in terms of the frame $\vec{\xi}_1, \vec{\xi}_2, \vec{\xi}_3$. By a change of tensor product basis we obtain

$$v^{ij} \vec{e}_i \otimes \vec{e}_j = v^{ij} \eta_i^r \eta_j^s \vec{\xi}_r \otimes \vec{\xi}_s \quad (8)$$

Now the coefficients in the tensor product basis of frame vectors are replaced by their approximates. This yields

$$\begin{aligned} \overline{(v^{ij} \eta_i^r \eta_j^s)} \vec{\xi}_r \otimes \vec{\xi}_s &= (1 - \delta_r^3) v^{ij} \eta_i^r \eta_j^s \vec{\xi}_r \otimes \vec{\xi}_s \\ &= \sum_{r=1}^2 v^{ij} \eta_i^r \eta_j^s \vec{\xi}_r \otimes \vec{\xi}_s \end{aligned} \quad (9)$$

A transformation back into the tensor product basis of the coordinate tangents is needed so that the approximation can be properly inserted into Navier-Stokes equations which were expressed in terms of the coordinate system. We obtain

$$\begin{aligned}
 \widetilde{(\nu^{ij} \eta_i^r \eta_j^s)} \vec{\xi}_r \otimes \vec{\xi}_s &= \sum_{r=1}^2 \nu^{ij} \eta_i^r \eta_j^s \xi_r^m \xi_s^k \vec{e}_m \otimes \vec{e}_k \\
 &= \sum_{r=1}^2 \nu^{ij} \eta_i^r \xi_r^m \delta_j^k \vec{e}_m \otimes \vec{e}_k \\
 &= \sum_{r=1}^2 \nu^{ik} \eta_i^r \xi_r^m \vec{e}_m \otimes \vec{e}_k \\
 &= \{ \delta_i^m - \eta_i^3 \xi_3^m \} \nu^{ik} \vec{e}_m \otimes \vec{e}_k
 \end{aligned} \tag{10}$$

and, therefore, new coefficients of viscous stress ω^{mk} defined by

$$\begin{aligned}
 \omega^{mk} &= \widetilde{\nu}^{mk} \\
 &= \{ \delta_i^m - \eta_i^3 \xi_3^m \} \nu^{ik} \\
 &= \{ \delta_i^m - \eta_i^3 \xi_3^m \} \{ \alpha_j^{ik} \nu^j + \beta_j^{ik} \frac{\partial \nu^j}{\partial y^k} \}
 \end{aligned} \tag{11}$$

The approximation is now complete when this is inserted into the equations.

As a special case, suppose that the primary direction vector field is given by the y^3 coordinate curves. Then, $\vec{\xi}_3 = \vec{e}_3$. This is easily extended to an orthogonal triad by setting $\vec{\xi}_2 = \vec{e}^2$ and $\vec{\xi}_1 = g_{31} \vec{e}_3 - g_{33} \vec{e}_1$. In the present tube-like geometry, we would take y^1 , y^2 , and y^3 for the angular, radial, and axial variables, respectively, as illustrated in Fig. 3.

Our approximation to the Navier-Stokes equations can be written explicitly in the conservation law form given previously. The time-averaging for turbulent fluctuations, however, requires some additional notation. Specifically, the dependent variables are represented as the sum of a time-averaged quantity denoted by a straight overbar (-) and an instantaneous fluctuating quantity denoted by a curved overbar (~).

After time-averaging, the equations become

$$\frac{\partial}{\partial y^i} \left[(\bar{\rho} \bar{v}^i + \bar{\rho} \bar{v}^i) \sqrt{g} \right] = 0 \quad (12a)$$

for continuity, and

$$\begin{aligned} \frac{\partial}{\partial y^j} \left[(\bar{\rho} \bar{v}^i \bar{v}^j + \bar{\rho} \bar{v}^i \bar{v}^j + \bar{\rho} \bar{v}^i \bar{v}^j + \bar{\rho} \bar{v}^j \bar{v}^i \right. \\ \left. + g^{ij} \bar{p} + \bar{g}^{ij}) \frac{\partial x^s}{\partial y^i} \sqrt{g} \right] = 0 \end{aligned} \quad (12b)$$

for momentum. The triple cross correlation terms have been neglected. Since the remaining components of Reynolds stress are coefficients in the tensor product basis $\bar{e}_i \otimes \bar{e}_j$, they can be expressed in any needed form via a change of tensor product basis.

Note that since the new stress tensor is not symmetric the index ordering in the viscous stress is important. In fact, if by mistake it should become inverted, then the primary direction momentum balance would have no viscous contributions at all. This, however, would be a false result since significant shearing stresses would be neglected. One can most easily examine this situation via the stress cube (Fig. 2) by considering any cartesian system with one coordinate aligned with the primary direction \bar{e}_3 . With proper index alignment one gets precisely the desired equations. However, with the incorrect alignment the axial momentum equation is inviscid. Thus considerable care must be taken so that one does not inadvertently apply symmetry to the nonsymmetric stress tensor derived here.

For entirely supersonic flows, the approximate equations (Eqs. (12a) and (12b)), together with boundary and initial conditions can be solved by forward marching integration in the x direction without any assumptions about the pressure field, as was demonstrated by McDonald & Briley (Ref. 18) for laminar flow in rectangular jets.

THE NUMERICAL METHOD

Overview

In the previous section we derived a system of equations in which the time-like derivative of the solution vector was expressed implicitly. This occurred because time-like derivative was applied to a flux vector instead of the solution vector directly. The association with the word flux is a direct result of the general Stokes theorem and the conservation law form of Eqs. (12a) and (12b). Since the time-like direction is the spatial marching direction and since the equations were derived from the steady-state Navier-Stokes equations, (4a) and (4b), the flux vector is a nontrivial function of the solution. Consequently one is faced with the problem of constructing a numerical method that is sufficiently general to solve the general system of equations of the previous section. Since time-like variations are nontrivial, a second order solution is preferred.

The method used is based on an implicit scheme which is potentially stable for large step sizes. Thus as a practical matter, stability restrictions which limit the axial step size relative to the transverse mesh spacing and which become prohibitive for even locally refined meshes (e.g., in laminar sublayers) are not a factor in making the calculations. The general approach is to employ an implicit difference formulation and to linearize the implicit equations by expansion about the solution at the most recent axial location. Terms in the difference equations are then grouped by coordinate direction and one of the available alternating-direction implicit (ADI) or splitting techniques is used to reduce the multidimensional difference equations to a sequence of one-dimensional equations. These linear one-dimensional difference equations can be written in block-tridiagonal or a closely related matrix form and solved efficiently without iteration by standard block elimination techniques. The general solution procedure is quite flexible in matters of detail such as the type and order accuracy of the difference approximations and the particular scheme for splitting multidimensional difference approximations. Based on previous experience of the authors, however, it is believed that the consistent use of a formal linearization procedure, which incidentally requires the solution of coupled difference equations in most instances, is a major factor in realizing the potential favorable stability properties generally attributed to implicit difference schemes.

After modeling Reynolds stresses the governing equations of the previous section can be solved by the general approach to be presented herein which is motivated by the previous work of McDonald and Briley (Ref. 25). Unlike the earlier work, the present algorithm achieves second order accuracy for the forward marching direction using only two levels of storage as opposed to three. In addition, the present analysis is developed directly on tensor-like objects which contain

a considerable amount of generality and hence applicability. Further developments come with the construction of an implicit-explicit shifting function which can be used to well-condition an ill-conditioned transformation by creating a diagonally dominant (Varga, Ref. 26) and hence numerically solvable system. Other applications of implicit-explicit shifting occur when it is desired to cast the implicit difference equations in a form suitable for ADI splitting along coordinate directions. Here one shifts all mixed implicit transverse derivatives to the explicit side. This avoids extra ADI sweeps or an increase in the matrix banded structures of the individual sweeps.

The System of Equations

In keeping with the viewpoint of maintaining generality, the numerical method shall be developed in a slightly more general context than is actually needed. Specifically, M-th order N-dimensional systems of the form

$$\frac{\partial H_i}{\partial t} = F_i \quad (13a)$$

are to be solved for a solution $(\varphi_\ell) = (\varphi_1, \dots, \varphi_N)$ where

$$H_i = H_i(\tau, x_j, F_{i\alpha}) = H_i(\tau, x_j, p_{i\alpha}(\lambda, x_k, \varphi_\ell)) \quad (13b)$$

$$F_i = F_i(\tau, x_j, q_{i\alpha}) = F_i(\tau, x_j, q_{i\alpha}(\lambda, x_k, \varphi_\ell)) \quad (13c)$$

$$\tau(t) = \lambda(t) = t = \text{time-like variable} \quad (13d)$$

$$(x_j) = (x_1, \dots, x_N) = \text{spatial variables} \quad (13e)$$

for $1 \leq i, j, k, \ell \leq N$ and a multi-index $\alpha = (\alpha_1, \dots, \alpha_{2M})$ with integers α_j . The reader should note that there has been a use of a compressed notation to indicate functional dependence. The power of this notation is easily observed from the expansion.

$$p_{i\alpha}(\lambda, x_k, \varphi_\ell) = p_{i\alpha}(\lambda, x_1, x_2, \dots, x_N, \varphi_1, \varphi_2, \dots, \varphi_N) \quad (14)$$

In addition, this notation avoids the confusion that can result when chain rule expansions produce Jacobian-like objects of varying dimensions. This should be obvious from the form $H_i(\tau, x_j, p_{i\alpha})$ since (x_j) and $(p_{i\alpha})$ are vectors of generally unequal lengths. This notation should, of course, be distinguished from the Einstein summation convention of summing like indices which is in the context of sums of products as opposed to the argument listings here. The spatial

derivatives and the dependence upon the solution vector (φ_ℓ) are all contained in the specification of the functions $p_{i\alpha}$ and $q_{i\alpha}$ in (13b) and (13c). Specifically, one has

$$p_{i\alpha} = D_{\alpha_1} G_{i\alpha_{M+1}} \dots D_{\alpha_M} G_{i\alpha_{2M}} \quad (15a)$$

where

$$D_{\alpha_j} = \begin{cases} \frac{\partial}{\partial x_{\alpha_j}} & \text{for } \alpha_j = k, 2, \dots, N \\ \text{Identity} & \text{for } \alpha_j = 0 \end{cases} \quad (15b)$$

and

$$G_{i\alpha_{M+j}} = G_{i\alpha_{M+j}}(\lambda, x_k, \varphi_\ell) \quad (15c)$$

The form of $q_{i\alpha}$ is similar but with different functions $G_{i\alpha_{M+j}}$. It should be noticed that all of these specific forms can be expanded by successive applications of the chain and Leibnitz rules. If these expansions were taken to the point where only derivatives of the form $D_{\beta_1} \dots D_{\beta_M} \varphi_\ell$ would appear then both $p_{i\alpha}$ and $q_{i\alpha}$ could be replaced by expressions of the form $D_\alpha \varphi_\ell$ where $D_\alpha = D_{\alpha_1} \dots D_{\alpha_M}$ and $\alpha = (\alpha_1, \dots, \alpha_M, \alpha_{M+1}, 0, \dots, 0)$ with $0 \leq \alpha_j \leq N$ and $\alpha_{M+1} \neq 0$. In particular, one would have the solution vector $\varphi_{\alpha_{N+1}} = p_{i\alpha} = q_{i\alpha}$ for $\alpha = (0, \dots, 0, \alpha_{M+1}, 0, \dots, 0)$ and derivatives of $\varphi_{\alpha_{N+1}}$ up to order M as α varied otherwise. This simplified functional form for $p_{i\alpha}$ and $q_{i\alpha}$ would certainly make the theoretical discussion easier; however, the computational complexity of the problem would generally be increased. In many cases a natural grouping of functions $p_{i\alpha}$ and $q_{i\alpha}$ occurs. Such groupings are easy to spot in the general fluid equations (12a) to (12b). The above expansion and redefinition of $p_{i\alpha}$ and $q_{i\alpha}$ would generally increase the number of terms in the equations. Each of these terms would require roughly the same number of operations involved in linearizations and differencing as was required in the original. Thus, the operation count would generally go up in a direct proportion to the increase in number of terms. Consequently, it is preferable to stay with the theoretically more cumbersome form of equations (15) which produce a computationally more efficient scheme. Since the derivative operators with respect to λ , φ_ℓ , and t all commute with the operator D_{α_j} of (15b); the differentiation of $p_{i\alpha}$ and $q_{i\alpha}$ with respect to λ , φ_ℓ , or t is easily seen to obey the chain rule. Thus, one can treat the operator functions $p_{i\alpha}$ and $q_{i\alpha}$ as ordinary functions in the variables λ and φ_ℓ .

From the chain rule, the system of partial differential equations (13) can be rewritten in the form

$$A_{i\ell} \frac{\partial \varphi_\ell}{\partial t} = F_i - \frac{\partial H_i}{\partial \tau} - \frac{\partial H_i}{\partial p_{i\alpha}} \frac{\partial p_{i\alpha}}{\partial \lambda} \quad (16a)$$

where

$$A_{i\ell} = \frac{\partial H_i}{\partial p_{i\alpha}} \frac{\partial p_{i\alpha}}{\partial \varphi_\ell} = \frac{\partial H_i}{\partial \varphi_\ell} \quad (16b)$$

is just the Jacobian of the flux (H_i) in the solution vector (φ_ℓ). If the matrix ($A_{i\ell}$) represents a nonsingular linear transformation A , then one can directly solve for the time-like derivatives of the entire solution vector. Otherwise one must consider a system of lower rank and with constraining relations. Under a change of basis equations (16) can be rewritten in an equivalent form where the linear transformation A is represented by a matrix with r linearly independent rows and $N-r$ rows of zeros where r is the rank of A . The last $N-r$ rows of the transformed equations correspond to the nullity of A and hence involve no time-like derivatives. Consequently one can consider these to be constraining relationships which can be used to eliminate the last $N-r$ rows of the solution vector in the first r equations. If this is possible, then one has reduced the original system of N equations in N unknowns to an equivalent system of r equations in r unknowns. These systems will be called reducible systems. This terminology corresponds with the matrix terminology since a discretization of the system would lead to reducible matrices (Varga, Ref. 26). If the system is reducible at each point (t, x_j) with a continuous transformation of basis, then the system will be called a solvable system. Only solvable systems shall be considered here; and, in fact, without loss of generality one can assume that A is nonsingular for otherwise the reduced system would just produce a smaller nonsingular version of A which would be solved in the same manner. With this consideration one obtains

$$s_j \equiv \frac{\partial \varphi_j}{\partial t} = B_{ji} \left[F_i - \frac{\partial H_i}{\partial \tau} - \frac{\partial H_i}{\partial p_{i\alpha}} \frac{\partial p_{i\alpha}}{\partial \lambda} \right] \quad (17)$$

where the matrix (B_{ji}) is the inverse of (A_{ik}) and the notation s_j is introduced to denote the value of the time-like derivative of the j^{th} component of the solution vector that is determined directly by the system of partial differential equations.

The Numerical Scheme

Time-like variations of the system of equations (13) are generally nontrivial. This is evident on examination of the system of approximate Navier-Stokes equations developed in the previous chapter. There one has a time-like direction associated with the spatial direction which is then used to march the solution. The remaining directions form what is generally referred to as a transverse surface which is often taken as a transverse plane. As the solution is marched the geometry of the problem changes as the bounding contours in transverse surfaces generate the flow region in a generally nontrivial fashion. Thus one has considerably more opportunities for error growth than if the flow region had no variations in the time-like direction at all. With this motivation it is preferable to develop a second order scheme as opposed to a first order one.

The numerical scheme that is developed here is a second order generalization of the classical Crank-Nicolson scheme. In the well-centered framework of Crank-Nicolson one has

$$\frac{H_i^{n+1} - H_i^n}{h} = F_i^{n+\frac{1}{2}} + O(h^2) \quad (18)$$

where $h = t^{n+1} - t^n$ and all superscripts are used to denote time-like evaluations. The reader may also notice that all other indices in this section were carefully taken to be subscripts. In this way no confusion can result. One now must evaluate both sides of the Crank-Nicolson equation (18) and preserve second order accuracy. From a Taylor expansion of the right hand side about level n one obtains

$$F_i^{n+\frac{1}{2}} = F_i^n + \left\{ \frac{\partial F_i}{\partial \tau} + \frac{\partial F_i}{\partial q_{i\alpha}} \left[\frac{\partial q_{i\alpha}}{\partial \lambda} + \frac{\partial q_{i\alpha}}{\partial \varphi_\ell} \frac{\partial \varphi_\ell}{\partial t} \right] \right\}^n \frac{h}{2} + O(h^2) \quad (19)$$

where the chain rule has been used. The n -level evaluations in the first order piece are straight forward with the exception of the quantity $(\partial \varphi_\ell / \partial t)^n$. This can be either evaluated by a finite difference or directly from the differential equations with s_j^n of equation (17). If the latter approach is taken, then the implicit character of the basic Crank-Nicolson scheme is lost. Thus a finite difference shall be used. Since the term itself is first order, the simple first order forward difference is sufficient. Thus one obtains

$$F_i^{n+\frac{1}{2}} = F_i^n + \left\{ \left(\frac{\partial F_i}{\partial \tau} \right)^n + \left(\frac{\partial F_i}{\partial q_{i\alpha}} \right)^n \left(\frac{\partial q_{i\alpha}}{\partial \lambda} \right)^n \right\} \frac{h}{2} \\ + \left(\frac{\partial F_i}{\partial q_{i\alpha}} \right)^n \left(\frac{\partial q_{i\alpha}}{\partial \varphi_\ell} \right)^n (\varphi_\ell^{n+1} - \varphi_\ell^n) + o(h^2) \quad (20)$$

On the left hand side of the Crank-Nicolson equation (18) one must evaluate a time-like difference quotient of fluxes. This is obtained by a Taylor Series expansion about the n -level. To break the calculation up into manageable pieces it is best to first expand each of the $(n+\frac{1}{2})$ -level derivatives about level n . In so doing one obtains the finite difference

$$\left(\frac{\partial \varphi_\ell}{\partial t} \right)^{n+\frac{1}{2}} = \frac{\varphi_\ell^{n+1} - \varphi_\ell^n}{h} + o(h^2), \quad (21a)$$

the Taylor Series expansion

$$\left(\frac{\partial H_i}{\partial \tau} \right)^{n+\frac{1}{2}} = \left(\frac{\partial H_i}{\partial \tau} \right)^n + \left(\frac{\partial^2 H_i}{\partial t \partial \tau} \right)^n \frac{h}{2} + o(h^2) \\ = \left(\frac{\partial H_i}{\partial \tau} \right)^n + \left\{ \frac{\partial^2 H_i}{\partial \tau^2} + \frac{\partial^2 H_i}{\partial p_{i\alpha} \partial \tau} \left[\frac{\partial p_{i\alpha}}{\partial \lambda} + \frac{\partial p_{i\alpha}}{\partial \varphi_j} \frac{\partial \varphi_j}{\partial t} \right] \right\}^n \frac{h}{2} \\ + o(h^2) \quad (21b)$$

and the similar expansions

$$\left(\frac{\partial H_i}{\partial p_{i\alpha}} \right)^{n+\frac{1}{2}} = \left(\frac{\partial H_i}{\partial p_{i\alpha}} \right)^n + \left\{ \frac{\partial^2 H_i}{\partial \tau \partial p_{i\alpha}} + \frac{\partial^2 H_i}{\partial p_{i\beta} \partial p_{i\alpha}} \left[\frac{\partial p_{i\beta}}{\partial \lambda} + \frac{\partial p_{i\beta}}{\partial \varphi_j} \frac{\partial \varphi_j}{\partial t} \right] \right\}^n \frac{h}{2} \\ + o(h^2) \quad (21c)$$

$$\left(\frac{\partial p_{i\alpha}}{\partial \lambda} \right)^{n+\frac{1}{2}} = \left(\frac{\partial p_{i\alpha}}{\partial \lambda} \right)^n + \left\{ \frac{\partial^2 p_{i\alpha}}{\partial \lambda^2} + \frac{\partial^2 p_{i\alpha}}{\partial \varphi_j \partial \lambda} \frac{\partial \varphi_j}{\partial t} \right\}^n \frac{h}{2} + o(h^2) \quad (21d)$$

and

$$\left(\frac{\partial p_{i\alpha}}{\partial \varphi_\ell}\right)^{n+\frac{1}{2}} = \left(\frac{\partial p_{i\alpha}}{\partial \varphi_\ell}\right)^n + \left\{ \frac{\partial^2 p_{i\alpha}}{\partial \lambda \partial \varphi_\ell} + \frac{\partial^2 p_{i\alpha}}{\partial \varphi_j \partial \varphi_\ell} \frac{\partial \varphi_j}{\partial t} \right\}^n \frac{h}{2} + o(h^2) \quad (21e)$$

The time-like difference of equation (18) is now obtained by a direct substitution of equations (21) followed by an absorption of second order terms into the collection $O(h^2)$. The result is given by

$$\begin{aligned} \frac{H_i^{n+1} - H_i^n}{h} &= \left(\frac{\partial H_i}{\partial \tau}\right)^n + \left\{ \frac{\partial^2 H_i}{\partial \tau^2} + \frac{\partial^2 H_i}{\partial p_{i\alpha} \partial \tau} \left[\frac{\partial p_{i\alpha}}{\partial \lambda} + \frac{\partial p_{i\alpha}}{\partial \varphi_j} \frac{\partial \varphi_j}{\partial t} \right] \right\}^n \frac{h}{2} \\ &+ \left(\frac{\partial H_i}{\partial p_{i\alpha}}\right)^n \left\{ \left(\frac{\partial p_{i\alpha}}{\partial \lambda}\right)^n + \left[\frac{\partial^2 p_{i\alpha}}{\partial \lambda^2} + \frac{\partial^2 p_{i\alpha}}{\partial \varphi_j \partial \lambda} \frac{\partial \varphi_j}{\partial t} \right]^n \frac{h}{2} \right. \\ &+ \left. \left(\frac{\partial p_{i\alpha}}{\partial \varphi_\ell} + \left[\frac{\partial^2 p_{i\alpha}}{\partial \lambda \partial \varphi_\ell} + \frac{\partial^2 p_{i\alpha}}{\partial \varphi_j \partial \varphi_\ell} \frac{\partial \varphi_j}{\partial t} \right] \frac{h}{2} \right)^n \left(\frac{\varphi_\ell^{n+1} - \varphi_\ell^n}{h} \right) \right\} \\ &+ \left\{ \frac{\partial^2 H_i}{\partial \tau \partial p_{i\alpha}} + \frac{\partial^2 H_i}{\partial p_{i\beta} \partial p_{i\alpha}} \left[\frac{\partial p_{i\beta}}{\partial \lambda} + \frac{\partial p_{i\beta}}{\partial \varphi_j} \frac{\partial \varphi_j}{\partial t} \right] \right\}^n \frac{h}{2} \left\{ \left(\frac{\partial p_{i\alpha}}{\partial \lambda}\right)^n \right. \\ &+ \left. \left(\frac{\partial p_{i\alpha}}{\partial \varphi_\ell}\right)^n \left(\frac{\varphi_\ell^{n+1} - \varphi_\ell^n}{h} \right) \right\} + o(h^2) \end{aligned} \quad (22)$$

Now it is best to regroup the above into n -level time-like derivatives of φ_j and time-like differences in φ_ℓ with coefficients ordered by powers of h . This regrouping yields the form

$$\begin{aligned} \frac{H_i^{n+1} - H_i^n}{h} &= a_i^n + b_{ij}^n \left(\frac{\partial \varphi_j}{\partial t} \right)^n + c_{i\ell}^n \left(\frac{\varphi_\ell^{n+1} - \varphi_\ell^n}{h} \right) + d_{ij\ell}^n \left(\frac{\partial \varphi_j}{\partial t} \right)^n \left(\frac{\varphi_\ell^{n+1} - \varphi_\ell^n}{h} \right) \\ &+ o(h^2) \end{aligned} \quad (23)$$

where

$$a_i = \frac{\partial H_i}{\partial \tau} + \frac{\partial H_i}{\partial p_{i\alpha}} \frac{\partial p_{i\alpha}}{\partial \lambda} + \frac{h}{2} \left[\frac{\partial H_i}{\partial \tau^2} + 2 \frac{\partial^2 H_i}{\partial p_{i\alpha} \partial \tau} \frac{\partial p_{i\alpha}}{\partial \lambda} + \frac{\partial H_i}{\partial p_{i\alpha}} \frac{\partial^2 p_{i\alpha}}{\partial \lambda^2} + \frac{\partial^2 H_i}{\partial p_{i\beta} \partial p_{i\alpha}} \frac{\partial p_{i\beta}}{\partial \lambda} \frac{\partial p_{i\alpha}}{\partial \lambda} \right] \quad (24a)$$

$$b_{ij} = \frac{h}{2} \left[\frac{\partial H_i}{\partial p_{i\alpha}} \frac{\partial^2 p_{i\alpha}}{\partial \lambda \partial \varphi_j} + \left(\frac{\partial^2 H_i}{\partial \tau \partial p_{i\alpha}} + \frac{\partial^2 H_i}{\partial p_{i\beta} \partial p_{i\alpha}} \frac{\partial p_{i\beta}}{\partial \lambda} \right) \frac{\partial p_{i\alpha}}{\partial \varphi_j} \right] \quad (24b)$$

$$c_{i\ell} = \frac{\partial H_i}{\partial p_{i\alpha}} \frac{\partial p_{i\alpha}}{\partial \varphi_\ell} + b_{i\ell} \quad (24c)$$

and

$$d_{ij\ell} = \left[\frac{\partial H_i}{\partial p_{i\alpha}} \frac{\partial^2 p_{i\alpha}}{\partial \varphi_j \partial \varphi_\ell} + \frac{\partial^2 H_i}{\partial p_{i\beta} \partial p_{i\alpha}} \frac{\partial p_{i\beta}}{\partial \varphi_j} \frac{\partial p_{i\alpha}}{\partial \varphi_\ell} \right] \frac{h}{2} \quad (24d)$$

From successive applications of the chain rule in conjunction with the Leibnitz rule, the coefficients can be condensed into the simple forms

$$a_i = \frac{\partial H_i}{\partial T} + \frac{h}{2} \frac{\partial^2 H_i}{\partial T^2} \quad (25a)$$

$$b_{ij} = \frac{h}{2} \frac{\partial^2 H_i}{\partial T \partial \varphi_j} \quad (25b)$$

$$c_{ij} = \frac{\partial H_i}{\partial \varphi_j} + b_{ij} \quad (25c)$$

and

$$d_{ijk} = \frac{h}{2} \frac{\partial^2 H_i}{\partial \varphi_j \partial \varphi_k} \quad (25d)$$

where

$$\frac{\partial}{\partial T} \equiv \frac{\partial}{\partial \tau} + \frac{\partial}{\partial \lambda} \quad (25e)$$

Time-like derivatives of quantities other than the solution vector φ_j are given by derivatives with respect to T . Such quantities, for example, are often items that are built up from the metric information when the equations of motion are expressed in some curvilinear coordinate system. The derivatives with respect to T occur only in the coefficients a_i , b_{ij} , and c_{ij} . When the time-like dependence is on the solution vector φ_j alone, the coefficients a_i and b_{ij} both obviously vanish and the coefficient c_{ij} is just the Jacobian of H_i . The expression for d_{ijk} is independent of T -derivatives and is easily identified as the product of $h/2$ and the Hessian of H_i .

To maintain second order accuracy the derivative $\frac{\partial \varphi_j}{\partial t}^n$ associated with the d_{ijl}^n -terms in equation (23) cannot be evaluated with a forward difference; for then, the quantities φ_l^{n+1} would appear in products of the form $\varphi_j^{n+1} \varphi_l^{n+1}$ and thus linearity would be lost. Consequently, one is left with two options. First, one may take a simple backwards difference to a level $(n-1)$ in the time-like variable. This difference represents the derivative to first order; and since the coefficient d_{ijl}^n already contains a factor of h , one has obtained second order accuracy. This was the option taken by McDonald and Briley (Ref. 25). The resulting scheme is, however, a three level scheme. In some problems storage is the critical factor; and in such cases, a two level scheme is much more desirable than a three level one. This motivates the second option. The idea is simply to evaluate the derivative directly from the original system of differential equations. Thus from equation (17) one has

$$s_j = \frac{\partial \varphi_j}{\partial t} = B_{ji} \left[F_i - \frac{\partial H_i}{\partial T} \right] \quad (26)$$

in terms of the T-derivative. From a direct substitution of this expression into the d_{ijl}^n -terms of equation (23) one obtains the representation

$$\begin{aligned} \frac{H_i^{n+1} - H_i^n}{h} = & a_i^n + b_{ij}^n \left(\frac{\partial \varphi_j}{\partial t} \right)^n + (c_{il}^n + d_{ijl}^n s_j^n) \left(\frac{\varphi_l^{n+1} - \varphi_l^n}{h} \right) \\ & + O(h^2) \end{aligned} \quad (27)$$

for the time-like flux difference on the left-hand side. Under either of the above options one has not yet finished the representation of this time-like flux difference since the n -level derivatives $\left(\frac{\partial \varphi_j}{\partial t} \right)^n$ associated with the b_{ij}^n -terms still remain

to be considered. Since coefficients b_{ij}^n contain a factor of h one can represent these derivatives by either a first order difference or a direct substitution of s_j^n . Unlike the d_{ijl}^n -terms there are no $(n+1)$ -level complications here and consequently only the simple first order forward difference need be considered. The representation of these terms, however, is not unique. For any n -level coefficient e_{ij}^n that is in $O(h)$ one has

$$e_{ij}^n \left[s_j^n - \left(\frac{\varphi_j^{n+1} - \varphi_j^n}{h} \right) \right] = 0 + O(h^2) \quad (28)$$

which can be added to equation (23) without changing the order. Now if one uses the forward difference for the b_{ij}^n -terms and adds equation (28) to equation (27), then one obtains the time-like flux difference representation

$$\frac{H_i^{n+1} - H_i^n}{h} = a_i^n - e_{il}^n s_l^n + \left[b_{il}^n + e_{il}^n + c_{il}^n + d_{ijl}^n s_j^n \right] \left(\frac{\varphi_l^{n+1} - \varphi_l^n}{h} \right) + o(h^2) \quad (29)$$

With $e_{il}^n = 0$ the effect is to represent b_{ij}^n -terms with a finite difference; and with $e_{il}^n = -b_{il}^n$ the direct substitution of s_l^n is used. In between there are an infinite number of possibilities. In effect this arbitrariness of e_{il}^n provides one with a degree of freedom that can be used to shift terms between implicit and explicit parts of the representation. The advantage here is that terms can be shifted towards the implicit side to insure diagonal dominance and hence invertibility of the implicit scheme. In addition, unwanted implicit terms can be shifted to make ADI-splitting easier. For these reasons, the function e_{il}^n shall be called an implicit-explicit shifter.

Both sides of the Crank-Nicolson equations (18) have been suitably approximated to second order with right and left hand sides being given by equations (20) and (29) respectively. By direct substitution one has the second order scheme

$$a_i^n - e_{il}^n s_l^n + \left[b_{il}^n + e_{il}^n + c_{il}^n + d_{ijl}^n s_j^n \right] \frac{\psi_l^{n+1}}{h} = F_i^n + \left\{ \left(\frac{\partial F_i}{\partial \tau} \right)^n + \left(\frac{\partial F_i}{\partial q_{i\alpha}} \right)^n \left(\frac{\partial q_{i\alpha}}{\partial \lambda} \right)^n \right\} \frac{h}{2} + \left(\frac{\partial F_i}{\partial q_{i\alpha}} \right)^n \left(\frac{\partial q_{i\alpha}}{\partial \varphi_l} \right)^n \psi_l^{n+1} \quad (30)$$

where $\psi_l^{n+1} = \varphi_l^{n+1} - \varphi_l^n$. From a multiplication by h , the notation of equation (25e), and the chain rule one obtains the form

$$\left[b_{il} + e_{il} + c_{il} + d_{ijl} s_j - \frac{h}{2} \frac{\partial F_i}{\partial \varphi_l} \right]^n \psi_l^{n+1} = h \left[F_i + \frac{h}{2} \frac{\partial F_i}{\partial \tau} - a_i - e_{il} s_l \right]^n \quad (31)$$

where the strength of the implicit coupling is controlled by the first order function e_{il} . While this function can be taken to extreme settings, it is usually taken as zero unless mixed derivatives occur or diagonal dominance is lost. The spatial differences are easily inserted into equation (31) by the mere replacement of the spatial differential operators D_k of equation (15b) with the difference operators Δ_k which are defined by

$$\Delta_k = \begin{cases} \sum_{i=-r}^s W_k(i) E_k(i) & \text{for } 0 < k < N \\ E_k(0) & \text{for } k = 0 \end{cases} \quad (32)$$

where $E_k(i)$ is the evaluation map on the position designated by translation of the k th grid variable by i grid points and where $W_k(i)$ is the associated finite difference weight. One easily notes that $E_k(0)$ is the identity. When the weights $W_k(i)$ are taken to give second order spatial accuracy in the interior and on the boundary the overall scheme of equation (31) is second order. Second order accuracy at interior points with a uniform mesh is achieved by setting $r=s=1$, $W_k(0)=0$ and

$$W_k(1) = -W_k(-1) = \frac{1}{(\Delta x)_k} \quad (33)$$

while taking $E_k(\pm 1)$ to be half point evaluations via two point averages.

The scheme of equation (31) produces a linear implicit system of equations which are efficiently solved by the classical ADI procedures given by Douglas and Gunn (Ref. 27). The ADI splitting is usually taken along coordinate directions. When this is the case mixed derivative terms are often eliminated on the implicit side by use of the function $e_{i\lambda}$ of equation (31).

It is often instructive to specialize from the general to the specific. In so doing one can consider the application of the scheme given in Eq. (31) to a system with $H_i = H_i(\varphi_i, \frac{\partial \varphi_k}{\partial y^\ell})$ and $F_i = F(\varphi_j, \frac{\partial \varphi_k}{\partial y^\ell})$. This system covers all equations that do not have time-like derivatives outside of the solution vector itself. In gas dynamics this type of system is obtained when a direct solution to the steady-state inviscid supersonic equations is desired in Cartesian coordinates.

From Eq. (25) one obtains $a_{ij} = b_{ij} = 0$, $c_{ij} = \frac{\partial H_i}{\partial \varphi_j}$, and $d_{ij\lambda} = \frac{h}{2} \frac{\partial^2 H_i}{\partial \varphi_j \partial \varphi_k}$; and from

Eq. (17) one has $s_j = B_{ji} F_i = (\frac{\partial H_\ell}{\partial \varphi_k})_{ji} F_i \equiv \frac{\partial \varphi_i}{\partial H_1} F_i$. By substitution into Eq. (31) one gets

$$\left[\frac{\partial H_1}{\partial \varphi_\ell} + \frac{h}{2} \frac{\partial^2 H_1}{\partial \varphi_j \partial \varphi_\ell} \frac{\partial \varphi_j}{\partial H_r} F_r - \frac{h}{2} \frac{\partial F_i}{\partial \varphi_\ell} \right]^n \psi_\ell^{n+1} = h F_i^n \quad (34)$$

with a choice of $e_{i\lambda} = 0$. If one had considered the time-dependent equations in primitive variables, then one would obtain $H_i = \varphi_i$ and hence the system

$$\left[\delta_\ell^i - \frac{h}{2} \frac{\partial F_i}{\partial \varphi_\ell} \right]^n \psi_\ell^{n+1} = h F_i^n \quad (35)$$

The further restriction to a single ordinary differential equation would lead to

$$\left(1 - \frac{h}{2} \frac{\partial F}{\partial \varphi}\right)^n \left(\frac{\varphi^{n+1} - \varphi^n}{h}\right) = F^n \quad (36)$$

or

$$\frac{\varphi^{n+1} - \varphi^n}{h} = \frac{1}{2} \left\{ F^n + \left[F^n + \left(\frac{\partial F}{\partial \varphi}\right)^n \left(\frac{\varphi^{n+1} - \varphi^n}{h}\right) h \right] \right\} \quad (37)$$

But now within the square parenthesis one has an approximation to F^{n+1} accurate to second order. If the system were linear in F , then one would have

$$\frac{\varphi^{n+1} - \varphi^n}{h} = \frac{F^n + F^{n+1}}{2} \quad (38)$$

which is exactly the Crank-Nicolson scheme.

THE COORDINATE SYSTEM

The Construction of Tube-like Coordinates

Tube-like coordinates will be constructed in general to provide a natural setting for the study of flows within, between, or outside of a set of prescribed tubes. The prescribed boundary tubes then become coordinate surfaces, and, as a result, the specification of fluid dynamic boundary conditions is greatly simplified. Although the equations of motion contain more terms than for a cartesian system, this does not add excessively to the run time of a program. In addition, there must be some control over the resolution of regions near bounding tubes so that the effects of wall curvature and the growth of attached boundary layers can be adequately treated. Such controls are obtained from the specification of coordinate distribution functions which shall appear only as parameters in the basic geometric construction of the coordinates. The basic geometry of the bounding tubes then provides the intrinsic constraints upon the coordinate construction. Since the primary goal is the computation of fluid flows within nontrivial geometries and not the development of coordinate systems per se, the coordinates will be kept as simple as possible, given the desired generality.

Considering various past successes of two-dimensional conformal mappings to obtain coordinates, one might naturally wish to obtain similar transformations for three-dimensions. Unfortunately, there is no three-dimensional theory of conformal transformations analogous to complex variables, and consequently, in three dimensions one is left with a complicated system of partial differential equations which generally would require numerical solution. To circumvent the considerable computational labor required for solution of such equations, a constructive process is used for the development of tube-like coordinates.

The first step in the construction of tube-like coordinates is to create a suitable family of two-dimensional surfaces which, in some sense, are transverse to a given centerline. If orthogonal coordinates are desired, then these surfaces would have to bend and flex as the tube would undergo changes in cross section at different centerline positions. In addition to the problem of constructing transverse surfaces which bend and flex, there is also the problem of constructing an orthogonal grid on a surface which has variations in Gaussian curvature, and hence, is not flat. This second problem, in fact, requires a more complicated construction than the first which in itself is not easy. Thus, the sheer magnitude of the work involved in the construction of orthogonal coordinates certainly would remove the desire for their use in fluid dynamic problems which undoubtedly would require less computation in nonorthogonal coordinates than in the construction of an orthogonal system alone. By contrast, if the transverse surfaces are selected to be two-dimensional planes, then the construction of coordinates is greatly simplified while the fluid dynamic computation is only marginally different due to coordinate nonorthogonality. Consequently the coordinate system that we shall construct will have planar transverse surfaces.

Since each planar transverse surface is a linear subspace of the real three-dimensional Euclidian vector space R^3 , any such plane can be completely specified by any two spanning linearly independent vectors in R^3 . The specification of the planar family of transverse surfaces is then a result of a construction of two vector fields along a given centerline curve in R^3 . The origin of each plane is chosen to coincide with the associated centerline point. (See Fig. 4.) To assure that the planes are always indeed transverse, it will be assumed that they are orthogonal to the centerline at their origins. Ultimately, tube-like surfaces will be generated by loops about the planar origins which deform in some way as we move along the centerline curve; in general, these tube-like surfaces will not intersect the transverse planes orthogonally. Thus, only the centerline direction determines the transverse nature of the cross sectional planes. Specifically, the centerline tangent vectors form a vector field which, at each point, is orthogonal to the plane of the two transverse vectors, and thus each centerline point carries a triple of linearly independent vectors. By the Gram-Schmidt orthogonalization procedure, each such triple of vectors can be made into an orthogonal set, and hence, an orthonormal set which is simply called a frame. Thus, tube-like coordinate systems are constructed from a specified centerline curve and an associated frame field. Now the basic question is whether there is a canonical construction of tube-like coordinate systems from either a given centerline or a given frame field. From the theory of space curves (Ref. 26), it is well known that for positive curvature and specified torsion there is a local one-to-one correspondence between frame fields and space curves which pass through a given point. Thus, for nonzero curvature, the centerline space curve has a canonical frame field which is known as the Frenet frame. Consequently, the coordinates will be derived from the Frenet frame when it exists. At centerline points of zero curvature, the Frenet frame is degenerate and must be treated specially.

Once the Frenet frame of the space curve $\vec{\gamma}$ has been established, the unit normal and binormal vectors \vec{V}_2 and \vec{V}_3 at each point of $\vec{\gamma}$ determine a transverse plane orthogonal to the unit tangent vector \vec{V}_1 . (See Fig. 5.) Relative to any such transverse plane, these vectors are also the standard orthonormal basis. Consequently, we can examine the plane separately from the curve, $\vec{\gamma}$, which will only appear as the point at the origin. In two dimensional functional terminology, the unit normal direction can be considered as the abscissa and the unit binormal as the ordinate; or more simply, as x and y axes, respectively. Since the tube-like coordinates are to be generated from some family of tubes encasing the space curve, $\vec{\gamma}$, a cross-sectional cut by a transverse plane produces within the plane a family of loops about the origin. We shall assume that each loop is representable by a strictly monotone radial function of angle. In this regard, a polar type of description is the most suitable. But, of course, the loops are usually more complicated than circles, and thus, we must replace the radius by a function L of both radial and angular variables r and θ . Furthermore, when noncircular loops bound a cross section of fluid, there are regions of varying wall curvature. In a numerical solution, it is desirable to put proportionately more mesh points in regions of higher curvature than in regions of less curvature. Consequently, an angular

distribution function, Θ , is a good replacement for the simple angular specification, θ , of simple polar coordinates. The net result is a generalization where polar coordinates are replaced by a pseudo-radius, r and pseudo-angle, θ . Since the loops generally vary from transverse plane to transverse plane, the pseudo-radii and angles must also be functions of axial location, t , on the centerline space curve, $\vec{\gamma}(t)$. Since the normal and binormal directions are usually functions only of the centerline curve, $\vec{\gamma}(t)$, our loops may have symmetries that do not reflect about either of these Frenet directions. Since the use of known symmetries is a great simplification in most problems, we need an option which allows one to define axes that can be aligned in an optimal way. This option is easily established from the specification of a function, $\Omega(t)$, which is a rigid rotation relative to the normal-binormal directions. To bring this development of tube-like coordinates within the framework of the preceding tensor derivations, we shall use the notation, $y^1 = \theta$, $y^2 = r$ and $y^3 = t$ for pseudo-angular, pseudo-radial, and axial variables. In this notation, we have thus far developed (1) a length factor, $L = L(y^1, y^2, y^3)$, which is a generalization of radius, (2) an angular distribution function, $\Theta = \Theta(y^1, y^3)$ which is a generalization of angle, (3) a rotation function, $\Omega = \Omega(y^3)$, and (4) the Frenet frame, $(\vec{V}_1, \vec{V}_2, \vec{V}_3) = (\vec{V}_1(y^3), \vec{V}_2(y^3), \vec{V}_3(y^3))$ upon which the coordinates are built. That the length factor, L , and the angular distribution function, Θ , give us a generalization of polar coordinates is obvious since polar coordinates are easily retrieved by taking $L(y^1, y^2, y^3) = y^2$ and $\Theta(y^1, y^3) = y^1$. It is also worth noting that the angular distribution function, Θ , was chosen to be independent of pseudo-radius, y^2 . Although it is not immediately evident, we have removed a considerable amount of potential computational complexity in the process of obtaining metric information by limiting the number of derivatives which must be computed. Furthermore, there is no real loss of flexibility in the construction of angular distribution functions. Since most commonly used analytic descriptions of loops are, in fact, controlled by a collection of parameters which depend only on axial location, y^3 , a knowledge of only these parameters is often sufficient for the construction of the angular distribution function. For example, if the loops were to consist of a family of concentric homogeneous ellipses, then the major and minor axes of the outermost ellipse would form a collection of two such parameters.

With the above functions and the Frenet frame, the class of tube-like coordinates comes directly out of the transformation

$$\vec{x} = \vec{\gamma} + L[\vec{V}_2 \cos \varphi + \vec{V}_3 \sin \varphi] \quad (39)$$

which transforms curvilinear coordinates, $\vec{\gamma} = (y^1, y^2, y^3)$ into cartesian coordinates $\vec{x} = (x^1, x^2, x^3)$ where

$$\varphi(y^1, y^3) = \Theta(y^1, y^3) + \Omega(y^3). \quad (40)$$

At each transverse location, y^3 , the space curve vector, $\vec{\gamma}$, translates the origin to the space curve. At a given pseudo-angle, y^1 , a unit vector, $\vec{V}_2 \cos \varphi + \vec{V}_3 \sin \varphi$, is determined by the sum, $\varphi = \Theta + \Omega$ of the radial distribution function, Θ , and the transverse rotation, Ω . This unit vector sweeps out a full 360 degs in the transverse plane as y^1 passes through all of its values. Hence, we could call this a direction pointer for the transverse plane. When this direction pointer is scaled by the length factor, L , we obtain a point of our transformation. Since the length factor depends on all three variables, any set of tube-like surfaces can be obtained provided, of course, that loops are representable by a strictly monotone radial function of angle and also that no two transverse cross sections are allowed to intersect.

In a geometric setting, the transformation is really an embedding of tube-like coordinate systems into three dimensional Euclidian space. An illustration is provided in Fig. 5. From the transformation, it is also easy to see that the surfaces of constant y^3 are the transverse planes, the surfaces of constant pseudo-angle, y^1 , are ruled surfaces generated from the centerline curve, $\vec{\gamma}$, and the surfaces of constant pseudo-radius, y^2 , are just the concentric tubes about the space curve, $\vec{\gamma}$. Separate illustrations of these various coordinate surfaces are given in Figs. 6a, 6b, and 6c, respectively.

The Length Factor

Within the structure of tube-like coordinates, the length factor contains the information needed both for the specification of basic geometry and for the distributional control of the flow region. The distributional control can be easily implemented by the use of pseudo-radial and angular distributions as merely parameters in the construction of the length factor. In this way, the basic geometry can be treated separately from the distributional aspects. The point of separation becomes especially evident when the process of length factor construction is broken down into a number of stages. Since the bounding tubes can be smoothly generated from bounding loops within each transverse plane, it is sufficient to temporarily restrict our analysis to a consideration of regions between bounding loops within a transverse plane. For our tube-like coordinates, we have implicitly assumed that the nondegenerate bounding loops do not pass through the origin and are contractable along radial lines emanating from the origin. Thus, we do not allow bounding loops to intersect a radial line more than once. Consequently, each bounding loop γ_1 can be expressed in terms of polar coordinates (r, θ) as the product of a single valued radial function $F_1(\theta)$ and the unit vector $(\cos \theta, \sin \theta)$. With this polar description the contraction process effectively reduces to a one-dimensional process. Specifically it is a process between the coefficients of the unit vector $(\cos \theta, \sin \theta)$. For a given set of loops $\gamma_1, \dots, \gamma_k$ any sufficiently smooth interpolation process between the coefficients will be satisfactory. If we assume that no two tubes join within the flow region, then the flow region is divisible into subregions with no more than two bounding tubes. The interpolation process for two bounding loops γ_1 , and γ_2 is, therefore, all that is usually needed; and is given by the simple homotopy

$$H(\theta, r) = L(\theta, r) (\cos \theta, \sin \theta) \quad (41a)$$

with length factor

$$L(\theta, r) = rF_1(\theta) + (1-r) F_2(\theta) \quad (41b)$$

which takes $\gamma_2(\theta) = H(\theta, 0)$ uniformly and smoothly into $\gamma_1(\theta) = H(\theta, 1)$ as r goes from 0 to 1. (See Ref. 28.). This is illustrated in Fig. 7. If the loop γ_2 is degenerate then the coefficient $F_2(\theta)$ vanishes and the length factor reduces to $L(\theta, r) = rF_1(\theta)$, we thus have the cross section of a duct generated by one loop. By the continuity of L as a function of γ_2 , the duct generated by one loop γ_1 can be considered as a limit of annular type regions between loops γ_2 and γ_1 and γ_2 closes tightly upon the origin. This concept is often quite useful since the origin in coordinates generated from one loop suffer from the same singularity problem that occurs with simple polar coordinates. This singularity can be circumvented, however, by using an auxiliary loop γ_2 which is near enough to the origin to create a good approximation to the original region. To preserve overall accuracy in a numerical computation, $\|\gamma_2\| = \max_{\theta} F_2(\theta)$ must be less than the numerical truncation error. In fact, the well-defined limiting process would lead one to believe that there would be no problem at all in taking $\|\gamma_2\|$ arbitrarily small. But if $\|\gamma_2\|$ is taken within the region of machine roundoff error, then the singularity problem may reappear by default. Consequently, it is best to choose $\|\gamma_2\|$ to be much less than truncation errors but greater than roundoff errors.

The final stage of length factor construction is accomplished by a replacement of the polar coordinates r and θ by radial and angular distribution functions $R(r, t)$ and $\Theta(\theta, t)$ for axial location t . Now since R and Θ are to be the actual polar locations of a loop we must reinterpret r and θ as pseudo-radial and pseudo-angular locations on the same loop. Within this context the two-tube length factor becomes

$$L(\theta, r, t) = R(r, t) F_1(\Theta(\theta, t)) + [1-R(r, t)] F_2(\Theta(\theta, t)) \quad (42)$$

and the associated unit vector becomes

$$(\cos(\Theta(\theta, t) + \Omega(t)), \sin(\Theta(\theta, t) + \Omega(t))) \quad (43)$$

where the rotation $\Omega(t)$ of the Frenet frame has been included for completeness.

The Construction of Bounding Tubes

As the reader has just seen, the construction of tube-like coordinate systems relies upon the existence of smooth bounding tubes. When such tubes exist at the outset of a problem, the generation of coordinates is a straightforward application of the development above. However, if the bounding tubes are unknown at the outset, then they must be constructed in a smooth enough fashion. In such cases one is often given a discrete specification of a sequence of bounding loops which first must be fit with a smooth curve and then must be joined to form a smooth surface. This circumstance can often arise out of the convenience associated with the discrete specification of a surface by means of successive cross sectional cuts. If this data were to be given all in advance of the intended use of the coordinate system as a whole, then the smoothed cross sectional loops could be effectively joined by fitting them together with splines which can have interior knots corresponding to interior loops. However, it is often the case that discrete loop data is only generated one station in advance of the use of the coordinate system. This occurs, for example, when the problem is to solve for the viscous flow field outside of an ogival body when the flow is predominately supersonic. While the ogival body surface is known in advance, the location of the bow shock is not. Thus one considers the ogival body surface as the unknown outer tube which one wishes to use for the generation of tube-like coordinates to allow for the efficient computation of the fully viscous flow field. Since the flow field in a neighborhood of the bow shock is largely inviscid, an inviscid explicit solution is performed iteratively to obtain discretely the geometry of the bow shock at one station in advance of our known solution and coordinate system. One is now left with a fully developed bow shock surface preceded by a discrete cross sectional loop of bow shock data. The problem is to smoothly fit the loop and then smoothly join the result to obtain a smooth extension of the surface. Since fluctuations may arise from the discrete generation of the bow shock data, a least squares spline procedure is used to fit the loop with smoothness up to three continuous derivatives. This type of least-squares procedure has the distinct advantage of accurately representing the surface normal curvature along the loop. Now one has a loop $\gamma_{n+1}(\theta)$ at level $n+1$ and a bounding tube ending on a loop $\gamma_n(\theta)$ at level n where there are known derivatives in the axial direction t . One then attaches a surface which extends the tube from γ_n to γ_{n+1} with the smoothness of three continuous derivatives. The extension is accomplished with the tensor product form

$$p(\theta, t) = \sum_{j=0}^{r+1} f_j(t) \gamma_{n+1-j}(\theta) \quad (44)$$

which takes information back to loop γ_{n-r} . At the beginning r must be 1 since there are only two available loops. The process continues with r increasing until a desired maximum r value is obtained. From there on r is assumed to be constant.

Distribution Functions

When partial differential equations are discretized in terms of differences, the derivatives are replaced in some fashion by difference quotients. A simplification then leads to the difference equations that we solve. Implicitly in the discretization, however, is the assumption that derivatives are accurately estimated by secant lines. But then the exact solution may experience drastic variations in a short distance. Such solutions are said to have large gradients. In regions where the gradients are large, the approximation of derivatives by secants may be very poor unless the particular region is dissected into smaller regions which have reasonable secant approximations, a practice commonly known as mesh refinement. In fluid mechanics, the boundary layer of a viscous flow around or through an object is such a region.

Obviously, the necessary resolution could be accomplished by merely increasing the number of points in a uniform distribution; however, this would require excessive computer time and storage. Another alternative, known as the interface method, is to use a refined mesh only in the given region and then join it with the global mesh. An improved technique is to use coordinate distribution functions which smoothly distribute mesh points so that in some sense they are spaced in roughly an inverse proportion to the size of the gradients. Thus, regions of high gradients have proportionately more points than regions with smaller gradients. Unlike the interface method, the transition between different mesh lengths is made continuously, and as gradually as possible. Distributions are often used when the distributional transformation is applied to an independent variable of an existing transformation. The result is a new transformation obtained by composition. With this approach, the problem of mesh point distribution is replaced by the problem of selecting a suitable set of distribution functions within a transformation of coordinates. The problem is a nontrivial one since the distribution functions should depend upon the nature of the solution being computed but are determined in advance of the computation. Thus, some prior knowledge of the solution is required. In flows with large boundary layer separation or with adjacent dissimilar components, the critical region to be resolved is somewhere in the middle of the flow. But the location of such regions is often unknown at the outset of the problem. One method to overcome this difficulty in marching procedures is to create the distribution function at the next level based upon a knowledge of the solution at the present level. Care must be taken, however, to create a distribution function that is sufficiently smooth in the marching direction.

In many problems of practical interest, however, the regions that need resolution are known in advance. Typical examples are attached boundary layers and boundary layers that may have small separations or separation bubbles.

Within the framework of tube-like coordinate systems boundary layer resolution on the inner surface is accomplished by setting

$$R(r,t) = 1 + \frac{d}{\alpha} (r-1) \tanh \left[D \left(\frac{1-r}{1-\alpha} \right) \right] \quad (45)$$

where $d = d(t)$ is the estimated boundary layer growth, $\alpha = \alpha(t)$ is the desired proportion of mesh points in the boundary layer, and D is the hyperbolic damping factor. The boundary layer growth d gives the fraction of the flow region occupied by the boundary layer, α is usually taken as a constant, and D can be given a value of about 2. When r is small, the radial distribution of equation (45) reduces essentially to the line

$$R \approx \frac{d}{\alpha} r \quad (46)$$

which would have been chosen had we used the interface method. As r approaches unity the distribution Eq. (45) smoothly approaches unity as illustrated in Fig. 8.

Metric Data for Tube-Like Coordinates

The efficient generation of metric data is an important part of any solution procedure involving general curvilinear coordinates. Before a solution can be undertaken, the physical problem must be specified. Problem specification, however, involves the creation of boundary and initial data and the generation of the equations of motion with the associated boundary conditions. In addition, the solution may be monitored, examined, or put under physical constraints. In all of these tasks, the metric data is needed. A knowledge of the metric data is enough to completely specify the equations of motion and analyze the coordinate invariant directions for the specification of boundary and initial conditions. For very complicated geometries the equations of motion may contain an inordinate number of terms. However, if the equations are taken in tensor form, then the coefficients to terms can be constructed from the metric data with the construction process being performed on a computer. Once a non-trivial term is constructed, its contribution to the desired difference equations is computed before searching for the next non-trivial term. Sequentially, the process continues until all terms in the equations have given their contributions to the system of difference equations. Then, in the same fashion, we cycle through terms in the boundary conditions, sequentially adding in their respective contributions. The result is the desired set of difference equations, and the problem is effectively reduced to linear algebra. Note that with such methods there is no real need to write out the differential equations or complicated boundary conditions in detail. Thus, all we need to do is to generate the metric data and use it.

The metric data for tube-like coordinates can be obtained from the transformation

$$\vec{x} = \vec{Y} + L \{ \vec{V}_2 \cos \varphi + \vec{V}_3 \sin \varphi \} \quad (47)$$

sending tube-like coordinates $y = (y^1, y^2, y^3) = (\theta, r, t)$ into cartesian coordinates $x = (x^1, x^2, x^3)$ where $\varphi = \theta + \Omega$, and

$$\begin{aligned}
 \bar{Y} &= \bar{Y}(y^3) = \text{space curve center-line} \\
 \bar{V}_2 &= \bar{V}_2(y^3) = \text{unit normal vector} \\
 \bar{V}_3 &= \bar{V}_3(y^3) = \text{unit binormal vector} \\
 L &= L(y^1, y^2, y^3) = \text{length factor} \\
 \Theta &= \Theta(y^1, y^3) = \text{angular distribution} \\
 \Omega &= \Omega(y^3) = \text{rotation with respect to Frenet frame.}
 \end{aligned} \tag{48}$$

By differentiation of the coordinate transformation, we obtain the Jacobian transformation which leads directly to the transformation rules for tensor fields. These rules allow one to input, monitor, or extract basic information from a solution procedure involving transformed variables. The Jacobian Transformation is essentially obtained from the chain rule which yields

$$\bar{e}_i = \frac{\partial \bar{x}}{\partial y^i} = \frac{\partial x^j}{\partial y^i} \frac{\partial \bar{x}}{\partial x^j} = \frac{\partial x^j}{\partial y^i} \hat{u}_j \tag{49}$$

where \hat{u}_j is the standard orthonormal basis of constant vector fields, and \bar{e}_j is the natural basis of tangent vectors to coordinate curves. With a slight abuse of notation, we have used \bar{x} as a position vector in the definitions of \bar{e} and \hat{u} . However, nothing is lost since the covariant derivative of $\bar{x} = x^j \hat{u}_j$ is just the partial derivative of the x^j summed on \hat{u}_j . In terms of the notation

$$\hat{u}_1 = \begin{pmatrix} 1 \\ 0 \\ 0 \end{pmatrix}, \quad \hat{u}_2 = \begin{pmatrix} 0 \\ 1 \\ 0 \end{pmatrix}, \quad \hat{u}_3 = \begin{pmatrix} 0 \\ 0 \\ 1 \end{pmatrix} \tag{50}$$

we have

$$\bar{e}_i = \begin{pmatrix} \frac{\partial x^1}{\partial y^i} \\ \frac{\partial x^2}{\partial y^i} \\ \frac{\partial x^3}{\partial y^i} \end{pmatrix} \tag{51}$$

and hence the Jacobian matrix

$$(\vec{e}_1, \vec{e}_2, \vec{e}_3) = \begin{pmatrix} \frac{\partial x^1}{\partial y^1} & \frac{\partial x^1}{\partial y^2} & \frac{\partial x^1}{\partial y^3} \\ \frac{\partial x^2}{\partial y^1} & \frac{\partial x^2}{\partial y^2} & \frac{\partial x^2}{\partial y^3} \\ \frac{\partial x^3}{\partial y^1} & \frac{\partial x^3}{\partial y^2} & \frac{\partial x^3}{\partial y^3} \end{pmatrix} \quad (52)$$

Thus, to obtain the Jacobian transformation, we must calculate the natural coordinate-wise basis vectors \vec{e}_j .

For notational convenience, let derivatives of functions in only the axial variable y^3 be denoted by a dot; and in addition, let

$$L_{ijk} = \frac{\partial^{i+j+k} L}{(\partial y^1)^i (\partial y^2)^j (\partial y^3)^k} \quad (52a)$$

$$\Theta_{ij} = \frac{\partial^{i+j} \Theta}{(\partial y^1)^i (\partial y^3)^j} \quad (52b)$$

and

$$\varphi_{ij} = \frac{\partial^{i+j} \varphi}{(\partial y^1)^i (\partial y^3)^j} \quad (52c)$$

where $0 \leq i, j, k \leq 3$. By differentiation, we obtain

$$\vec{e}_1 = (L_{100} \cos \varphi - L_{010} \sin \varphi) \vec{V}_2 + (L_{100} \sin \varphi + L_{010} \cos \varphi) \vec{V}_3 \quad (53a)$$

$$\vec{e}_2 = (L_{010} \cos \varphi) \vec{V}_2 + (L_{010} \sin \varphi) \vec{V}_3 \quad (53b)$$

$$\begin{aligned} \vec{e}_3 = & \dot{s} \vec{V}_1 + L_{001} (\vec{V}_2 \cos \varphi + \vec{V}_3 \sin \varphi) \\ & + L (\dot{\vec{V}}_2 \cos \varphi + \dot{\vec{V}}_3 \sin \varphi - \vec{V}_2 \varphi_{01} \sin \varphi + \vec{V}_3 \varphi_{01} \cos \varphi) \end{aligned} \quad (53c)$$

Since the pseudo-angular vector \vec{e}_1 and the pseudo-radial vector \vec{e}_2 are linear combinations of the unit normal vector \vec{V}_2 and the unit binormal vector \vec{V}_3 , they both lie entirely within the transverse plane at axial location y^3 . But unlike \vec{e}_1 and \vec{e}_2 , the axial coordinate direction vector \vec{e}_3 is not expressed in terms of the basic Frenet frame. Thus, we cannot easily measure \vec{e}_3 relative to the transverse plane unless the y^3 -derivatives of unit normal and binormal vectors are expressed in terms of the Frenet frame. The necessary expressions are given by the last two Frenet formulas (Ref. 29) for the space curve γ ; namely,

$$\dot{\vec{V}}_2 = -\dot{s}\kappa \vec{V}_1 + \dot{s}\tau \vec{V}_3 \quad (54a)$$

and

$$\dot{\vec{V}}_3 = -\dot{s}\tau \vec{V}_2 \quad (54b)$$

where s is arc length, κ is curvature, and τ is torsion.

By substitution, we obtain

$$\vec{e}_3 = B\vec{V}_1 + (L_{001} \cos \varphi - LA \sin \varphi) \vec{V}_2 + (L_{001} \sin \varphi + LA \cos \varphi) \vec{V}_3 \quad (55)$$

where $A = \dot{s}\tau + \varphi_{01}$ and $B = \dot{s}(1 - \kappa L \cos \varphi)$. In summation, we have just obtained a change of basis $\vec{e}_i = b_i^j \vec{V}_j$ from the Frenet frame $\vec{V}_1, \vec{V}_2, \vec{V}_3$ to the natural basis of tube-like coordinate vectors $\vec{e}_1, \vec{e}_2, \vec{e}_3$. Previously, however, we found a change of basis $\vec{V}_j = a_j^m \hat{u}_m$ from the standard cartesian basis $\hat{u}_1, \hat{u}_2, \hat{u}_3$ to the Frenet frame. But then by composition we obtain the change of basis $\vec{e}_i = b_i^j a_j^m \hat{u}_m$ from cartesian tangent vectors to tube-like tangent vectors. By the identification developed above, the Jacobian elements are just

$$\frac{\partial x^m}{\partial y^i} = b_i^j a_j^m \quad (56)$$

for $i, m = 1, 2, 3$.

The metric tensor g_{ij} is obtained from the differential element of arc length $(ds)^2 = g_{ij} dy^i dy^j$. But alternatively, we have

$$(ds)^2 = d\vec{x} \cdot d\vec{x} = \left(\frac{\partial \vec{x}}{\partial y^i} dy^i \right) \cdot \left(\frac{\partial \vec{x}}{\partial y^j} dy^j \right) = \frac{\partial \vec{x}}{\partial y^i} \cdot \frac{\partial \vec{x}}{\partial y^j} dy^i dy^j = (\vec{e}_i \cdot \vec{e}_j) dy^i dy^j; \quad (57)$$

and hence, by linear independence $g_{ij} = \vec{e}_i \cdot \vec{e}_j$. That is, the metric tensor is computed by taking the dot products of the tube-like tangent vectors $\vec{e}_1, \vec{e}_2, \vec{e}_3$. This computation is most efficiently performed when the \vec{e}_i are expressed in terms of the Frenet frame. Since the Frenet frame is orthonormal, we have

$$g_{ij} = \vec{e}_i \cdot \vec{e}_j = (b_i^m \vec{V}_m) \cdot (b_j^\ell \vec{V}_\ell) = b_i^m b_j^\ell \vec{V}_m \cdot \vec{V}_\ell = b_i^m b_j^\ell \delta_{m\ell} = b_i^m b_j^m; \quad (58)$$

In particular, we obtain

$$g_{11} = L_{100}^2 + (L \Theta_{10})^2 \quad (59a)$$

$$g_{22} = L_{010}^2 \quad (59b)$$

$$g_{33} = B^2 + L_{001}^2 + (LA)^2 \quad (59c)$$

$$g_{12} = L_{100} L_{010} \quad (59d)$$

$$g_{13} = L_{100} L_{001} + L^2 \Theta_{10} A \quad (59e)$$

$$g_{23} = L_{010} L_{001} \quad (59f)$$

which by symmetry is the complete list. Note that the sines and cosines have disappeared as a result of cross-cancellation and the identity $\sin^2 \varphi + \cos^2 \varphi = 1$. Also note that the last three components listed are generally nontrivial off-diagonal entries. When any of these are non-zero, there is an angle other than 90° between the respective coordinate directions of the indices. For example, the cosine of the angle between the pseudo-angular direction \vec{e}_1 and the pseudo-radial direction \vec{e}_2 is given by the expression

$$\frac{g_{12}}{\sqrt{g_{11}g_{22}}} = \frac{L_{100}}{\sqrt{L_{100}^2 + (L\Theta_{10})^2}} \quad (60)$$

which vanishes only when $L_{100} = 0$. But when L_{100} vanishes, L is independent of angle and hence, the loops are circles. If, in addition, Θ is a uniform distribution, then the cross section is given by polar coordinates. In the same fashion, axially independent length factors would lead to the vanishing of g_{23} . If, in addition, the angular distribution and the rotation do not change along a straight axis, then g_{13} vanishes. In this case, the only non-orthogonality that can occur is in the transverse plane. If we combine all of the constraints above, then the tube-like coordinates become cylindrical coordinates.

The determinant of the metric can be easily obtained from elementary operations on determinants. That is,

$$\begin{aligned}
 g = \det (g_{ij}) &= L_{010}^2 \begin{vmatrix} 1 & L_{100} & L_{001} \\ L_{100} & L_{100}^2 + (L_{10}^\Theta)^2 & L_{100}L_{001} + L_{10}^{\Theta 2}A \\ L_{001} & L_{100}L_{001} + L_{10}^{\Theta 2}A & L_{001}^2 + (LA)^2 + B^2 \end{vmatrix} \\
 &= L_{010}^2 \begin{vmatrix} (L_{10}^\Theta)^2 & L_{10}^{\Theta 2}A \\ L_{10}^{\Theta 2}A & (LA)^2 + B^2 \end{vmatrix} \quad (61) \\
 &= (L L_{010} L_{10}^\Theta B)^2
 \end{aligned}$$

Alternatively, we also have

$$\begin{aligned}
 g = \det (g_{ij}) &= \det (\vec{e}_i \cdot \vec{e}_j) \\
 &= \det [(\vec{e}_1, \vec{e}_2, \vec{e}_3)^t (\vec{e}_1, \vec{e}_2, \vec{e}_3)] \quad (62) \\
 &= [\det (\vec{e}_1, \vec{e}_2, \vec{e}_3)]^2 \\
 &= |J|^2
 \end{aligned}$$

where J is the Jacobian of the transformation. Consequently, $J = L L_{010} \Theta_{10} B$. For the transformation to be nonsingular J must never vanish, and thus no factor in J can vanish. When L vanishes the transformation degenerates to the center line (Fig. 9a). When the pseudo-radial derivative L_{010} vanishes, two distinct coordinate loops coincide. This can happen by an intersection or a point of tangency (Fig. 9b). If Θ_{10} were to vanish, then the angular distribution Θ would fail to have the required monotonicity and hence a loop would be tangent to a radial line (Fig. 9c). Finally, if B vanishes, then two distinct transverse planes intersect (Fig. 9d). This leads to the restriction

$$L \cos \varphi \neq \frac{1}{K} \quad (63)$$

But the curve $L \cos \varphi = \frac{1}{K}$ is a line within a transverse plane (Fig. 9e). The line is parallel to the binormal axis and passes through the normal axis at $1/K$. As the transverse planes move throughout the centerline space curve, these lines generate a ruled surface. Our condition for nonsingularity is then that the space tubes must never come into contact with this ruled surface. Thus, space tubes must either lie below or beyond the surface. If they were to lie beyond the surface, however, then φ would be restricted to angles between -90° and 90° . But then if the tubes were generated by full transverse loops, they would have to possess a bottom and a top. This would imply that a given angle would yield a radial line with tangents to the loop and/or a multiple intersection with the loop. (Fig. 9f.) A singularity of this type is the same as a singularity arising from a nonmonotonic angular distribution. Consequently, the restriction is that the space tubes must lie below the ruled surface, or algebraically that

$$L \cos \varphi < \frac{1}{K} \quad (64)$$

The space-tubes are then assumed to encase the space curve $\vec{\gamma}$ and never come into contact with the above ruled surface. For tubes that have convex loops symmetrically centered about the space curve centerline, the restriction reduces to the statement that the length factor must be bounded in the normal direction by the radius of curvature (Fig. 9g). In general, if a tube fails to meet the inequality condition (Eq. 64), then it can be pushed off center until this condition is met. However, if the condition is so severe that the centerline must be taken extremely close to the normal side of a bounding tube, then coordinates will become unnaturally spaced. Since each loop (about this offset origin) intersects the normal line once on each side of the origin, the mesh spacing drastically changes. This would tend to cause an over-resolution on the normal side of the origin and an under-resolution on the opposite side. In such a case, it is best to generate the same bounding tube but with a new centerline with smaller curvature. This is always possible since we must only offset the old centerline in a convex direction which expands the curve rather than shrinking it. This is illustrated in Fig. 10.

If there are no coordinate singularities, then we can easily obtain the inverse of the metric. In a sequential order we have

$$g^{33} = \frac{1}{B^2} \quad (65a)$$

$$g^{13} = -\frac{A}{\Theta_{10}} g^{33} \quad (65b)$$

$$g^{11} = (g^{13B})^2 + \frac{1}{(L\Theta_{10})^2} \quad (65c)$$

$$g^{23} = \left(\frac{L_{100}}{L_{010}}\right) g^{13} + \left(\frac{L_{001}}{L_{010}}\right) g^{33} \quad (65d)$$

$$g^{12} = -\left(\frac{L_{001}}{L_{010}}\right) g^{13} - \left(\frac{L_{100}}{L_{010}}\right) g^{11} \quad (65e)$$

$$g^{22} = (Bg^{23})^2 + \left(\frac{L_{100}}{L_{010}}\right)^2 \left(\frac{1}{L\Theta_{10}}\right)^2 + \frac{1}{L^2_{010}} \quad (65f)$$

The \vec{e}_j -direction covariant derivative D_j of the vector \vec{e}_i is again a vector and hence is expressible in terms of the same basis $\vec{e}_1, \vec{e}_2, \vec{e}_3$. Specifically, we have

$$D_i e_j = \Gamma_{ij}^m e_m \quad (66)$$

where the coefficients Γ_{ij}^m are known as Christoffel symbols. This covariant derivative measures the rate of change of \vec{e}_j along a coordinate curve in the direction of \vec{e}_i . This coordinate curve is an integral curve of \vec{e}_i . It is obtained by fixing all except the i^{th} variable in the transformation. We shall assume that the covariant derivative is the natural one derivable from the metric. This is known as the Levi-Civita connection (Ref. 29). The Christoffel symbols for this covariant derivative are given by the formula

$$\Gamma_{ij}^k = \frac{g}{2} \frac{km}{\partial y^i \partial y^j \partial y^m} \left\{ \frac{\partial g_{mj}}{\partial y^i} + \frac{\partial g_{mi}}{\partial y^j} - \frac{\partial g_{ij}}{\partial y^m} \right\} \quad (67)$$

This formula is easily obtained by differentiating $g_{ij} = \vec{e}_i \cdot \vec{e}_j$ with respect to y^m , permuting all three of these indices, forming the sum in parenthesis, applying symmetry to the lower indices of the Christoffel symbols, and then applying the inverse metric. With some calculation, we obtain the non-zero Christoffel symbols directly from the above formula. For notational convenience, let

$$B_{ijk} = \frac{\partial^{i+j+k} B}{(\partial y^1)^i (\partial y^2)^j (\partial y^3)^k} \quad (68)$$

for $0 \leq i, j, k \leq 2$. Then we have

$$\begin{array}{l|l} \Gamma_{13}^3 = \frac{B_{100}}{B} & \Gamma_{23}^3 = \frac{B_{010}}{B} \\ \Gamma_{21}^1 = \frac{L_{010}}{L} & \Gamma_{22}^2 = \frac{L_{020}}{L_{010}} \\ \Gamma_{23}^1 = \frac{1}{\Theta_{10}} (\Gamma_{21}^1 - \Gamma_{13}^3) & \Gamma_{11}^1 = 2 \frac{L_{100}}{L} + \frac{\Theta_{20}}{\Theta_{10}} \end{array} \quad (69)$$

$$\begin{aligned} \Gamma_{31}^1 &= \frac{L_{001}}{L} + \frac{\Theta_{11}}{\Theta_{10}} + \frac{A}{\Theta_{10}} \left(\frac{L_{100}}{L} - \Gamma_{13}^3 \right) \\ \Gamma_{13}^2 &= \frac{L_{101}}{L_{010}} - \frac{L_{100}}{L_{010}} \left[\Gamma_{31}^1 + \frac{A}{\Theta_{10}} \Gamma_{13}^3 \right] - \frac{A \Theta_{10} L}{L_{010}} + g^{23} B_{100} B \\ \Gamma_{32}^2 &= \frac{1}{L_{010}} (L_{011} - \frac{A L_{110}}{\Theta_{10}}) + g^{23} B B_{010} \end{aligned}$$

$$\begin{aligned}\Gamma_{11}^2 &= \frac{1}{L_{010}} (L_{200} - L_{100} \Gamma_{11}^1 - L_{010}^2) \\ \Gamma_{33}^2 &= \frac{1}{L_{010}} \left\{ L_{002} - LA^2 - \frac{L_{100}}{\Theta_{10}} \left(\dot{A} + \frac{2 L_{001} A}{L} \right) \right\} \\ &\quad + \left(-g^{21} B_{100} - g^{22} B_{010} + g^{23} B_{001} \right) B\end{aligned}\tag{70}$$

$$\Gamma_{33}^1 = \frac{1}{\Theta_{10}} \left(\dot{A} + \frac{2 L_{001} A}{L} \right) + \left(-g^{11} B_{100} - g^{12} B_{010} + g^{13} B_{001} \right) B$$

and

$$\Gamma_{33}^3 = \left(-g^{31} B_{100} - g^{32} B_{010} + g^{33} B_{001} \right) B$$

When viscous calculations are to be done, we also need the derivatives of the above Christoffel symbols. This is a straight forward but tedious process. The derivative expressions are rather lengthy and we shall, therefore, not enumerate them. One may also note that the independence of Θ from r and of R from θ leads to a definite simplification in the Christoffel symbols. Had this independence not existed, then the above calculations would have been even more complex.

The geometric interpretation of the Christoffel symbols above is quite natural. For example, consider the special case when the centerline space curve is a straight line. Since the contravariant vector \vec{e}^3 is defined by the relation $\vec{e}^i \cdot \vec{e}_j = \delta_j^i$, it is perpendicular to the transverse plane. Consequently, \vec{e}^3 is a constant vector which is parallel to the straight centerline. But then the covariant derivative of a constant vector vanishes. By the Liebnitz rule for covariant derivatives, we then have

$$\begin{aligned}0 &= D_i (\delta_j^3) = D_i (\vec{e}_j \cdot \vec{e}^3) \\ &= (D_i \vec{e}_j) \cdot \vec{e}^3 + \vec{e}_j \cdot (D_i \vec{e}^3) \\ &= (\Gamma_{ij}^m \vec{e}_m) \cdot \vec{e}^3 + 0 \\ &= \Gamma_{ij}^m \delta_m^3 \\ &= \Gamma_{ij}^3\end{aligned}\tag{71}$$

for all $i, j = 1, 2, 3$. This fact can also be verified from our list of analytic expressions of Christoffel symbols. The geometric interpretation is that the covariant derivatives of natural basis vectors $\vec{e}_1, \vec{e}_2, \vec{e}_3$ have no axial projection and hence are transverse. In summary, we have just shown that with straight center-lines, no vector from the natural basis $\vec{e}_1, \vec{e}_2, \vec{e}_3$ can change in the axial direction. The only such vector with a non-trivial axial projection is, however, the natural vector \vec{e}_3 to axially generated coordinate curves. Consequently, the axial projection of \vec{e}_3 along such a coordinate curve is a constant as illustrated in Fig. 11.

TREATMENT OF THE BOW SHOCK

Although the shape of the body is specified at the start of the problem, the shape of the bow shock cannot be specified until effects of the body on the flow within the bow shock are evaluated. The shock shape is therefore evaluated at each new marching station based on information already computed. The shock surface is adopted as the outer coordinate surface and is used to determine the necessary metric information for the tube-like coordinates. The governing equations are then solved in the annular region between the ogival body and the bow shock by marching from one transverse plane to the next, proceeding in the nominally streamwise direction.

The bow shock is computed as a discontinuity satisfying the classical Rankine-Hugoniot relations. The intersection of this shock and a transverse computational plane is a loop represented by discrete grid points. Provided that a given grid point on this loop is outside the "zone of influence" of the neighboring points on the loop, the shock solution at the given point is independent of the solution at adjacent points. This "zone of influence" assumption is valid over a wide range of flow conditions and consequently is not a limiting assumption. Thus the shock radius $r_{n+1}(\theta)$ at each point in the $n+1$ transverse plane can be evaluated independently by a pointwise iteration procedure.

The iteration at each circumferential location in the $n+1$ plane proceeds by first locally extending the shock surface from the most recently evaluated transverse computational plane, n , to a point in the $n+1$ plane. The extension of the shock surface includes the point being evaluated in the $n+1$ plane, but does not extend circumferentially to the neighboring points. This extension is a first guess for the shock location at a circumferential point and hence for a point on the outer tube-like coordinate surface given by $r_{n+1}(\theta)$ in Eq. 44.

Given a guess at the shock location, the axial mass flux inside the shock can be computed by two methods. First, an application of the Rankine-Hugoniot conditions produces a value of the axial mass flux based only on the shock shape and the flow properties outside the shock. Second, an application of a compatibility condition produces a second value of this flux that depends only on the shock shape and the flow properties inside the shock. The shock location is then adjusted iteratively until the axial mass flux inside the shock computed by the two methods is the same. This iteration for the shock location is repeated at each of the circumferential grid points to produce a ring of discrete points at the $n+1$ station which collectively determine the shock surface. These discrete points must be represented by a continuous smooth curve to provide the information required to construct the coordinate system. For this purpose a least squares-spline curve fitting routine is employed.

REFERENCES

1. Rainbird, W. J.: Turbulent Boundary Layer Growth and Separation on a Yawed $12\frac{1}{2}^\circ$ Cone at Mach Numbers 1.8 and 4.25. AIAA Paper No. 68-98, January 1968.
2. Tracy, W. R.: Hypersonic Flow Over a Yawed Circular Cone. Mem. 69. Graduate Aeronautical Laboratories, California Institute of Technology, August 1963.
3. Stetson, K. F.: Experimental Results of Laminar Boundary Layer Separation on a Slender Cone at Angle of Attack at $M_\infty = 14.2$. ARL Report 71-0127.
4. Rainbird, W. J.: The External Flow Field About Yawed Circular Cones. AGARD Specialists Meeting, Hypersonic Boundary Layers and Flow Fields, London, May 1968.
5. Moretti, G.: Inviscid Flow Field Past a Pointed Cone at an Angle of Attack. General Applied Science Laboratory, Tech. Report 577, December 1965.
6. Moretti, G. and M. Abbett: A Time Dependent Computational Method for Blunt Body Flows. AIAA Journal, Vol. 4, No. 12, December 1966.
7. Lomax, H. and M. Inouye: Numerical Analysis of Flow Properties about Blunt Bodies Moving at Supersonic Speeds in an Equilibrium Gas. NASA TR R-204, 1964.
8. South, J. C. and E. B. Klunker: Methods for Calculating Nonlinear Conical Flows. NASA SP-228, 1969.
9. MacCormack, R. W. and R. F. Warming: Survey of Computational Methods for Three-Dimensional Inviscid Flows with Shocks. Advances in Numerical Fluid Dynamics, AGARD Lecture Series 64, Brussels, Belgium, February 1973.
10. Boerike, R. R.: The Laminar Boundary Layer on a Cone at Incidence in Supersonic Flow. AIAA Paper 70-48, January 1970.
11. Patankar, S. V. and D. B. Spalding: A Calculation Procedure for Heat, Mass, and Momentum Transfer in Three-Dimensional Parabolic Flows. Int. J. Heat and Mass Transfer, Vol. 15, 1972, p. 1787.
12. Caretto, L. S., R. M. Curr, and D. B. Spalding: Computational Methods in Applied Mechanics and Engineering, Vol. 1, 1973, p. 39.
13. Briley, W. R.: Numerical Method for Predicting Three-Dimensional Steady Viscous Flow in Ducts. Journal of Computational Physics, Vol. 14, 1974, p. 8.

REFERENCES (CONT'D)

14. Patankar, S. V., V. S. Pratap, and D. B. Spalding: Prediction of Laminar Flow and Heat Transfer in Helically Coiled Pipes. *Journal of Fluid Mechanics* Vol. 62, 1974, p. 539.
15. Rubin, S. G., and T. C. Lin: A Numerical Method for Three-Dimensional Viscous Flow: Application to the Hypersonic Leading Edge. *Journal of Computational Physics*, Vol. 9, p. 339, 1972.
16. Lin, T. C., and S. G. Rubin: Viscous Flow Over a Cone At Moderate Incidence. Part 2 Supersonic Boundary Layer. *Journal of Fluid Mechanics*, Vol. 59 Part 3, p. 593, 1973.
17. Helliwell, W. S., and S. C. Lubard: An Implicit Method for Three-Dimensional Viscous Flow With Application to Cones At Angle of Attack. *Computers and Fluids*, Vol. 3, p. 83, 1975.
18. Rakich, J. V., and S. C. Lubard: Numerical Computation of Viscous Flows on the Lee Side of Blunt Shapes Flying at Supersonic Speeds. *Aerodynamic Analyses Requiring Advanced Computers. Part 1. NASA SP-347*, 1975.
19. Briley, W. R. and H. McDonald: An Implicit Numerical Method for the Multi-dimensional Compressible Navier-Stokes Equations. *United Aircraft Research Laboratories Report M911363-6*, November 1973.
20. McDonald, H. and W. R. Briley: Three-Dimensional Supersonic Flow of a Viscous or Inviscid Gas. *United Aircraft Research Laboratories Report N111078-1*, November 1974.
21. Briley, W. R. and H. McDonald: Computation of Three-Dimensional Turbulent Subsonic Flow in Curved Passages. *United Aircraft Research Laboratories Report R75-911596-8*, March 1975.
22. Eiseman, P. R., H. McDonald, and W. R. Briley: A Method for Computing Three-Dimensional Viscous Diffuser Flows. *United Technologies Research Center Report R75-911737-1*, July 1975.
23. Eiseman, P. R.: The Numerical Solution of the Fluid Dynamic Equations in Curvilinear Coordinates. *Air Force Weapons Laboratory Technical Report AFWL-TR-73-172*, August 1973.
24. Hinze, J. O.: Turbulence, McGraw-Hill Book Company, Inc., New York, 1959.
25. McDonald, H. and W. R. Briley: Three Dimensional Supersonic Flow of a Viscous or Inviscid Gas. *Journal of Computational Physics*, Vol. 19, No. 2, October 1975.

REFERENCES (CONT'D)

26. Varga, R.: Matrix Iterative Analysis, Printice-Hall, Englewood Cliffs, N.J. 1962.
27. Douglas, J., and J. E. Gunn: A General Formulation of Alternating Direction Methods, Part I. Parabolic and Hyperbolic Problems. Numerische Mathematik, Vol. 6, 1964, p. 428.
28. Hu, S-T: Homotopy Theory. Academic Press, Inc., New York 1959.
29. Laugwitz, D.: Differential and Riemannian Geometry. Academic Press, Inc., New York 1965.

FIGURE 1. FLOW PAST AN OGIVE AT INCIDENCE

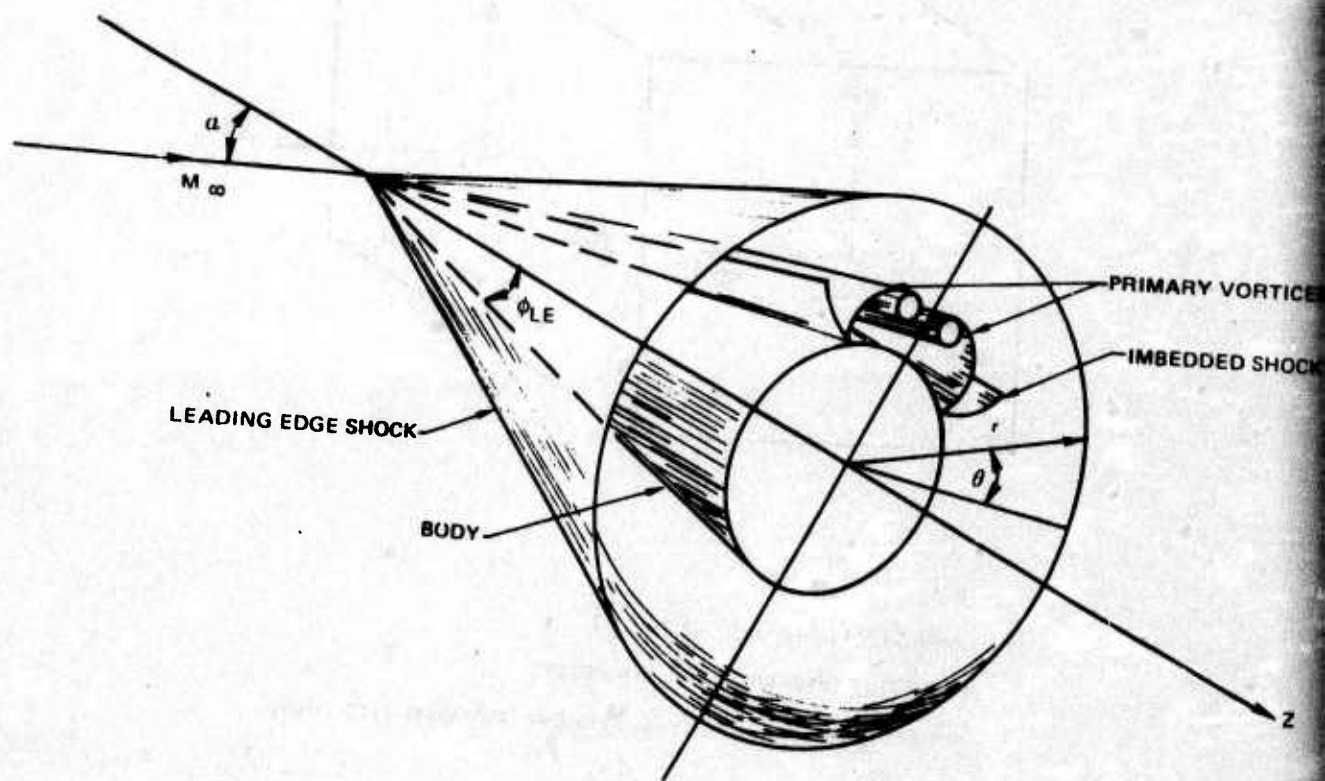
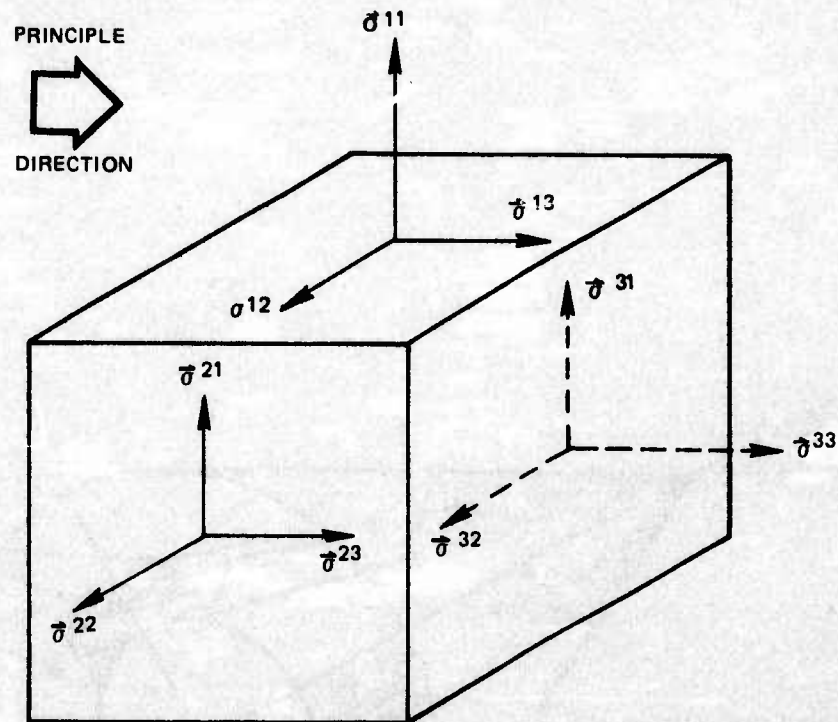


FIGURE 2. VISCOUS STRESS CUBE



$$\sigma_{ij} = \sigma_{ij} \xi_i \otimes \xi_j$$

APPROXIMATION = $\sigma_{3i} = 0$ FOR $i = 1, 2, 3$

RESULTING TENSOR IS NON-SYMMETRIC

THE EFFECTIVE DIFFERENTIAL ELEMENT IS A FIBER-LIKE THING

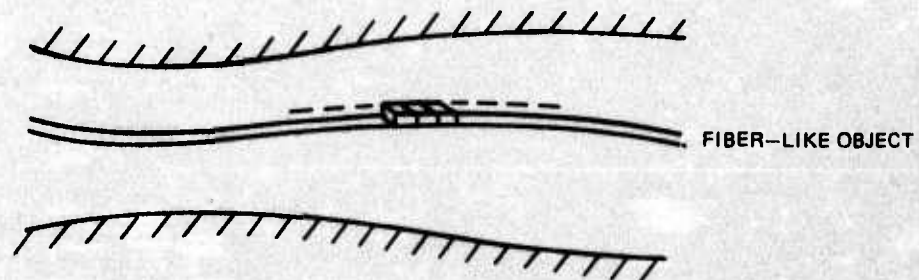
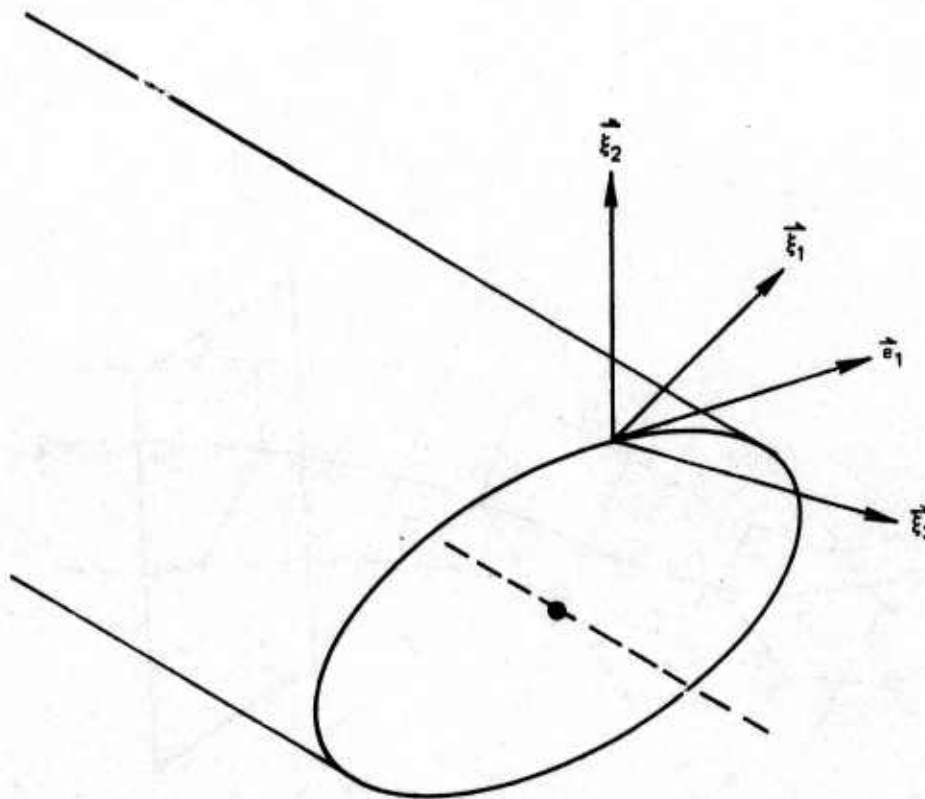


FIGURE 3. PRIMARY FLOW DIRECTION FROM THE COORDINATE SYSTEM



$$\vec{\xi}_3 = \vec{e}_3 = \text{PRIMARY DIRECTION}$$

$$\vec{\xi}_2 = \vec{e}_2$$

$$\vec{\xi}_1 = g_{13}\vec{e}_3 - g_{33}\vec{e}_1$$

FIGURE 4. GENERATION OF TRANSVERSE PLANES FROM TWO VECTOR FIELDS

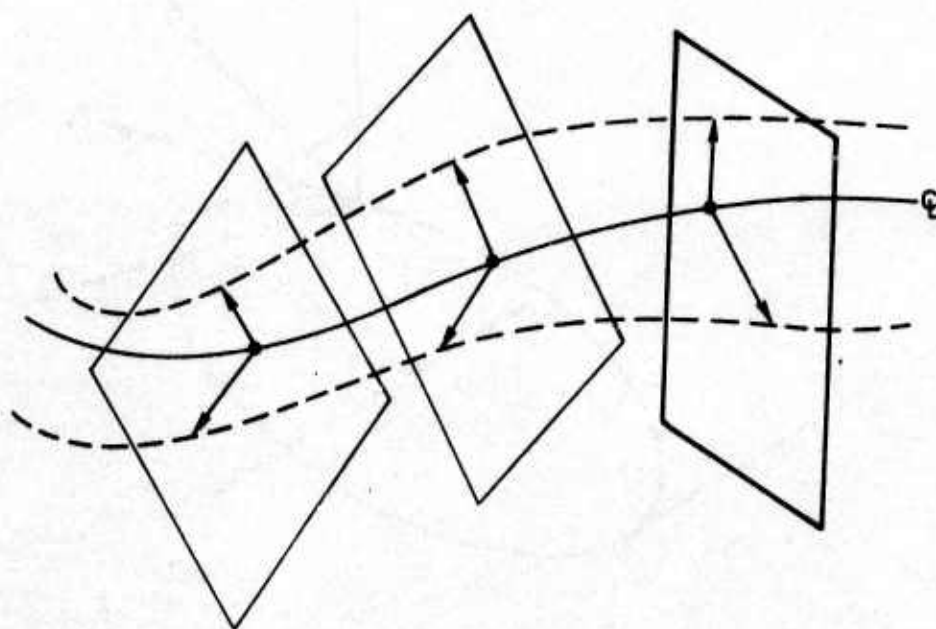


FIGURE 5. TRANSFORMATION AS AN EMBEDDING
INTO THREE DIMENSIONAL EUCLIDIAN SPACE

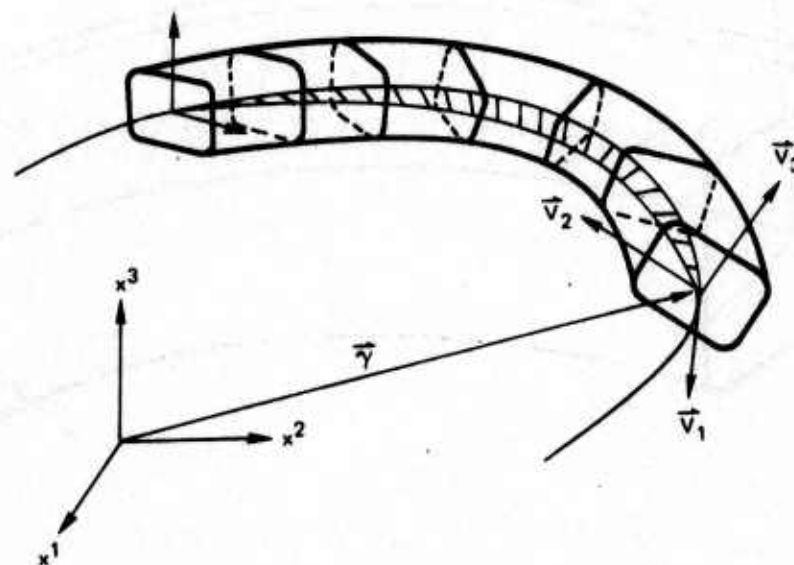


FIGURE 6a. TRANSVERSE PLANAR CUTS OF CONSTANT AXIAL LOCATION y^3

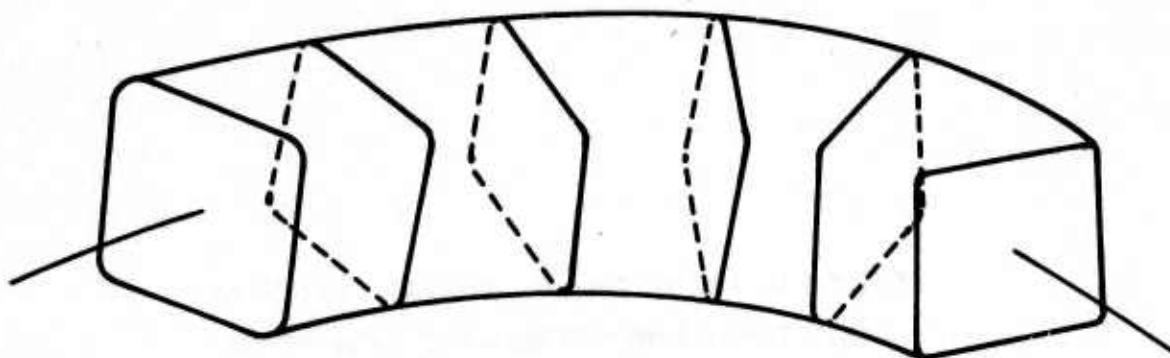


FIGURE 6b. RULED SURFACE OF CONSTANT PSEUDO-ANGLE y^1

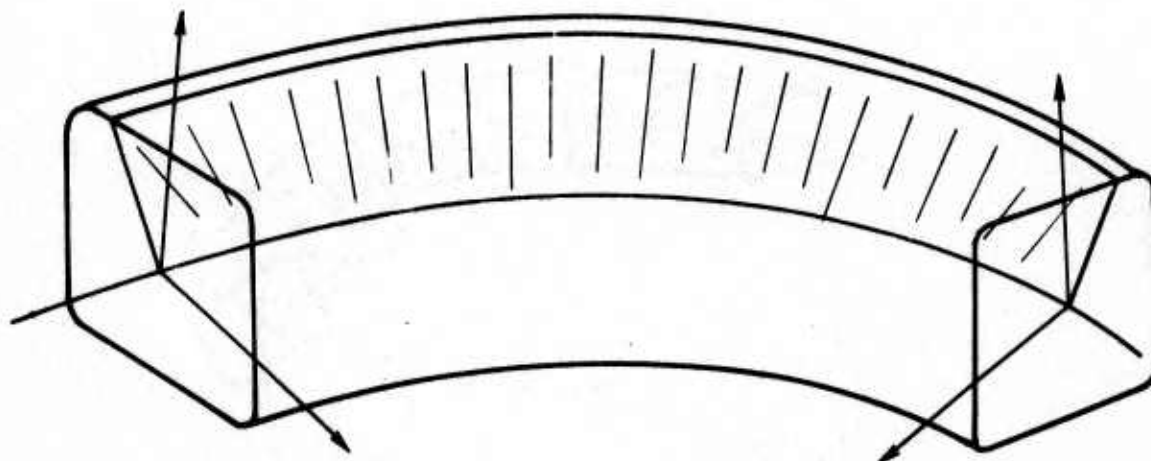


FIGURE 6c. TUBE-LIKE SURFACES OF CONSTANT PSEUDO-RADIUS y^2

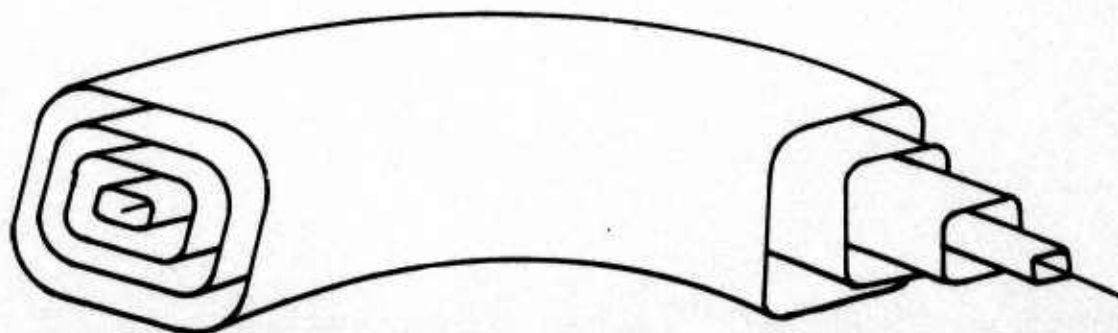


FIGURE 7. LINEAR HOMOTOPY BETWEEN TWO LOOPS

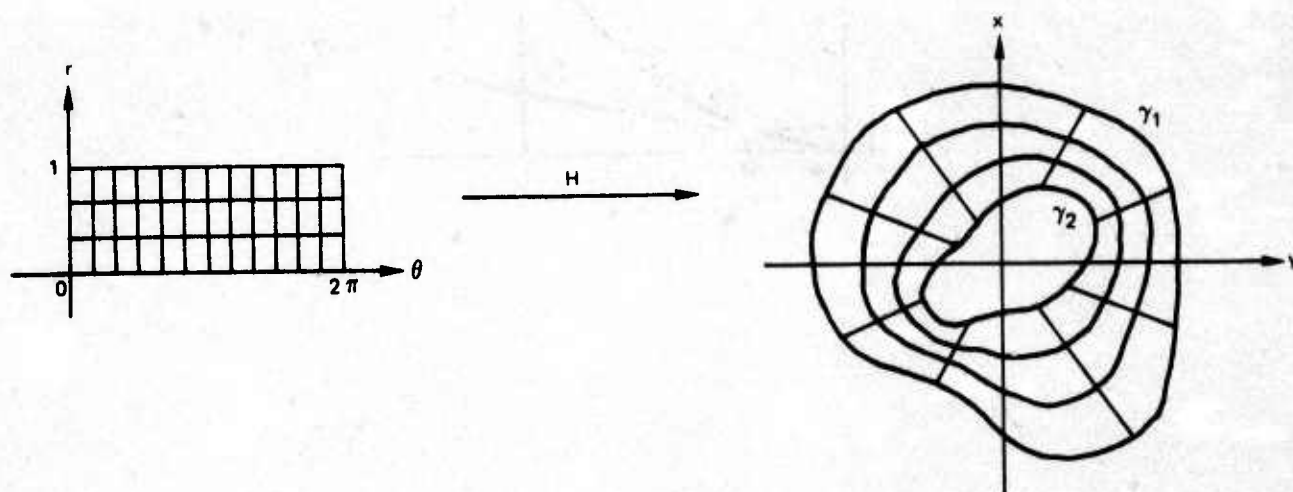


FIGURE 8. RADIAL DISTRIBUTION FUNCTION

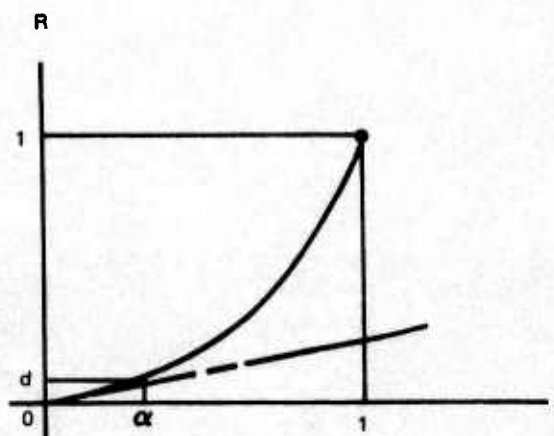


FIGURE 9. COORDINATE SINGULARITIES

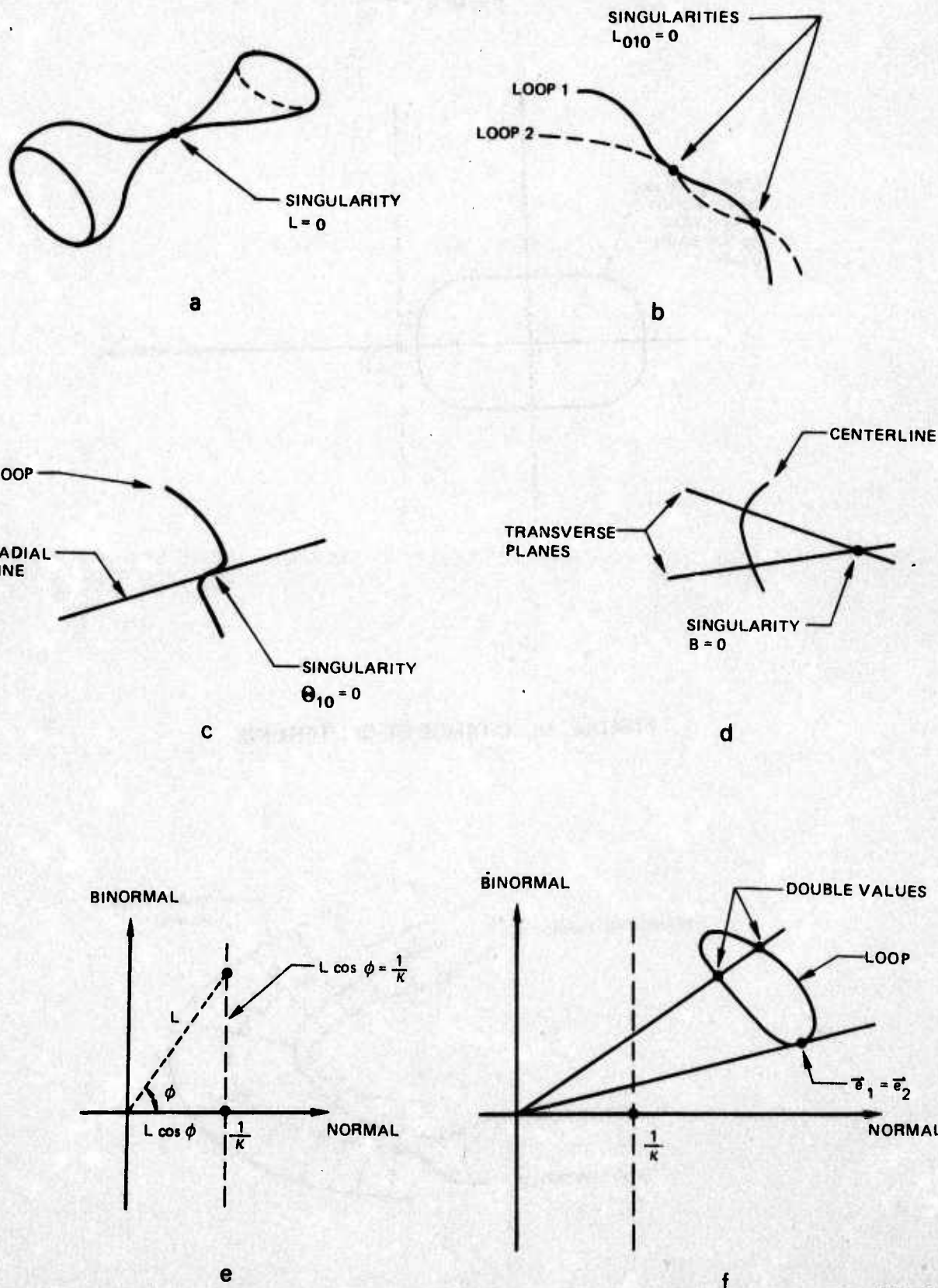


FIGURE 9g

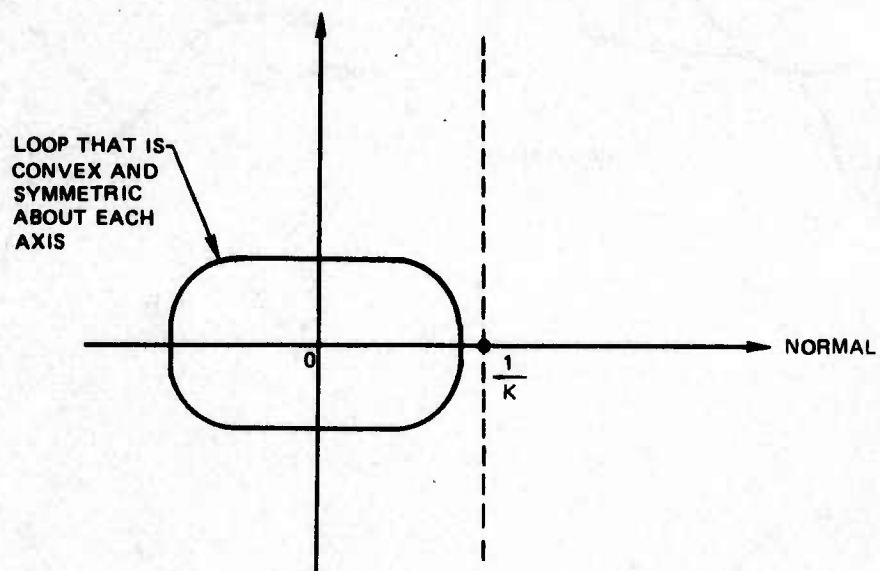


FIGURE 10. CHANGE OF CENTERLINE

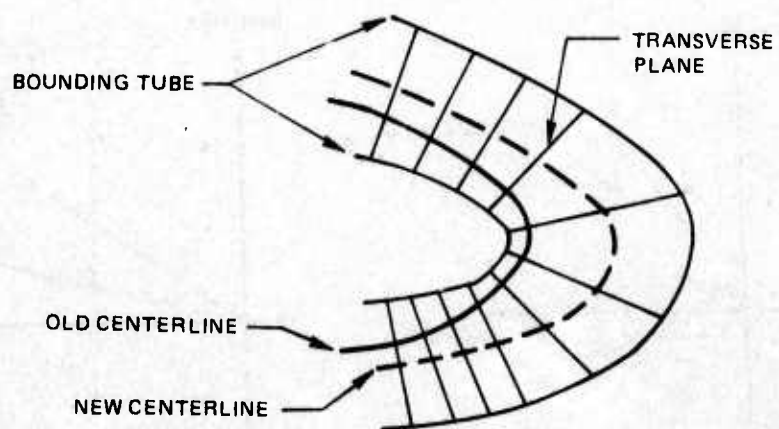
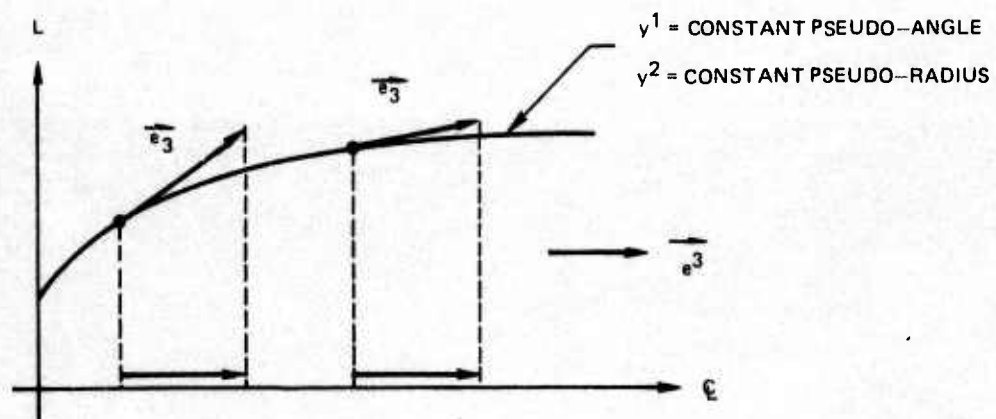



FIGURE 11. EQUAL PROJECTIONS



UNCLASSIFIED

SECURITY CLASSIFICATION OF THIS PAGE (When Data Entered)

REPORT DOCUMENTATION PAGE		READ INSTRUCTIONS BEFORE COMPLETING FORM
1. REPORT NUMBER (14) <u>UTRC -</u> <u>R76-912024-8</u>	2. GOVT ACCESSION NO.	3. RECIPIENT'S CATALOG NUMBER
4. TITLE (and Subtitle) (6) <u>Viscous</u> <u>A Method for Computing Three-Dimensional Flows</u> <u>Over an Ogival Body at Angle of Attack</u>	5. TYPE OF REPORT & PERIOD COVERED (9) <u>Final Report.</u> <u>484</u> (11) <u>Sep 1974-Oct 1975</u>	
7. AUTHOR(s) (10) <u>P. R. Eiseman</u> <u>R. Levy</u>	8. CONTRACT OR GRANT NUMBER(s) (15) <u>NO 0019-75-C-0097</u>	
9. PERFORMING ORGANIZATION NAME AND ADDRESS (1) <u>United Technologies Research Center</u> <u>Silver Lane</u> (2) <u>East Hartford, CT 06108</u>	10. PROGRAM ELEMENT, PROJECT, TASK AREA & WORK UNIT NUMBERS	
11. CONTROLLING OFFICE NAME AND ADDRESS	12. REPORT DATE (11) <u>February 1976</u>	
14. MONITORING AGENCY NAME & ADDRESS (if different from Controlling Office) <u>Department of the Navy</u> <u>Naval Air Systems Command</u> <u>Arlington, VA 22217</u>	13. NUMBER OF PAGES <u>62</u> (12) <u>65p.</u>	
15. SECURITY CLASS. (of this report) <u>UNCLASSIFIED</u>	15a. DECLASSIFICATION/DOWNGRADING SCHEDULE	
16. DISTRIBUTION STATEMENT (of this Report) 		
17. DISTRIBUTION STATEMENT (of the abstract entered in Block 20, if different from Report)		
18. SUPPLEMENTARY NOTES		
19. KEY WORDS (Continue on reverse side if necessary and identify by block number) <u>Ogival Body</u> <u>Bow Shock</u> <u>Tensor</u> <u>Tube-like Coordinates</u>		
20. ABSTRACT (Continue on reverse side if necessary and identify by block number) (U) A method for computing three-dimensional flow over an ogival body at an angle of attack is described. An approximate set of governing equations is derived for viscous flows which have a primary flow direction. The derivation is done in a coordinate independent manner, and the resulting equations are expressed in terms of tensors. In keeping with the inherent generality of the tensor formulation, a two-level second-order accurate		

DD FORM 1 JAN 73 1473

EDITION OF 1 NOV 65 IS OBSOLETE
S/N 0102-014-6601

UNCLASSIFIED

SECURITY CLASSIFICATION OF THIS PAGE (When Data Entered)

409252

NEXT Page

UNCLASSIFIED

SECURITY CLASSIFICATION OF THIS PAGE(When Data Entered)

→ marching procedure is derived for general tensor-like equations. With this procedure, a three-dimensional turbulent flow can be solved in any coordinate system by marching along the assumed primary flow direction. General tube-like coordinates are developed for a class of geometries applicable to flows between tubular surfaces. The coordinates are then particularized to the flow field bounded between an ogival body at angle of attack and its bow shock. Unlike the ogival body surface, the bow shock surface is not known in advance of the solution but instead must be computed as the solution develops. One marching step of the solution process is broken down into several steps. First, the bow shock surface is discretely extended by an iteration of explicit local inviscid solutions. The bow shock surface is then smoothly extended to provide a best fit to the discrete shock data. Tube-like coordinates are generated and finally the second order numerical scheme is applied to advance the fully viscous solution to the next station. →

UNCLASSIFIED